



TECHNICAL PAPER 37

HYGROTHERMAL PROPERTIES OF SCOTTISH MASONRY MATERIALS



HISTORIC
ENVIRONMENT
SCOTLAND

ÀRAINNEACHD
EACHDRAIDHEIL
ALBA

The views expressed in this Technical Paper are those of the authors and do not necessarily represent those of Historic Environment Scotland.

While every care has been taken in the preparation of this Technical Paper, Historic Environment Scotland specifically excludes any liability for errors, omissions or otherwise arising from its contents and readers must satisfy themselves as to the principles and practices described.

This Technical Paper is published by Historic Environment Scotland, the lead public body established to investigate, care and promote Scotland's historic environment. This publication is available digitally and free to download from the Historic Environment Scotland website:

www.historicenvironment.scot/technical-papers

All images unless otherwise noted are by Historic Environment Scotland.

This publication should be quoted as:
*Historic Environment Scotland Technical Paper 37:
Hygrothermal Properties of Scottish Masonry Materials.*
© Historic Environment Scotland 2022

Author: P.F.G. Banfill
Series Editor: Lila Angelaka

We welcome your comments. If you have any comments or queries about our Technical Papers or would like to suggest topics for future papers, please get in touch by email at TechnicalResearch@hes.scot

© Historic Environment Scotland 2022

You may re-use this information (excluding logos and



images) free of charge in any format or medium, under the terms of the Open Government Licence v3.0 except where otherwise stated.

To view this licence, visit

<http://nationalarchives.gov.uk/doc/open-government-licence/version/3>

or write to the Information Policy Team, The National Archives, Kew, London TW9 4DU,
or email: psi@nationalarchives.gov.uk

Where we have identified any third party copyright information you will need to obtain permission from the copyright holders concerned.

Any enquiries regarding this document should be sent to:

Historic Environment Scotland
Longmore House
Salisbury Place
Edinburgh
EH9 1SH
+44 (0) 131 668 8600
www.historicenvironment.scot

AUTHOR BIOGRAPHY

Phil Banfill is Professor Emeritus at Heriot-Watt University. Following a degree in chemistry, his 45 year university career saw him undertaking research and teaching across the whole range of construction materials.

He has published 200 papers and two books on such topics as cement and concrete science, traditional masonry, deterioration and durability, building conservation, energy utilisation in buildings, impacts of climate change, and issues of materials sustainability. He set up and for many years led Heriot-Watt's MSc in Building Conservation (Technology and Management), and subsequently established the Urban Energy Research Group.

Phil is a Chartered Chemist and a Fellow of the Royal Society of Chemistry. He has been a trustee of the Scottish Lime Centre Trust since 2006.



PREFACE

The modelling of the movement of water in various states in traditional mass walls with software packages has been established for some time. There are many tools which can be used, from relatively simple to more advanced. Their application has been considered in Historic Environment Scotland's Technical Paper 15: Assessing risks in insulation retrofits using hygrothermal software tools: Heat and moisture transport in internally insulated stone walls. The results of such modelling allow designers to consider and manage hygrothermal risk in any plans for upgrade to historic and traditional buildings. However, the materials information preloaded in these packages may not always reflect what was used in traditional construction and, therefore, may not always give accurate results for modelling traditional buildings. This Technical Paper has been commissioned to report on a series of basic tests carried out on a limited range of mortars and masonry types common in Scottish domestic buildings. The objective has been to begin to establish baseline material properties for traditional materials, so

that hygrothermal modelling can have more accurate inputs and give better outcomes that may reflect the beneficial properties of both traditional materials and construction techniques. While the number of stone and mortar samples investigated in this Technical Paper is limited, it covers the range of most common types encountered in Scotland and it will therefore be an improvement on the data available from the software defaults. From an early consideration of modelling outputs using this new data, it appears that, in most circumstances, modelled hygrothermal risk is reduced when using this specific data, as opposed to the default figures. This should give confidence to those in the retrofit sector that traditional wall constructions are durable and, in most cases, capable of being thermally upgraded without detriment to the masonry fabric and adjacent building components. It is anticipated that HES will deliver more hygrothermal testing to include a wider range of stone and mortar types to ensure the best simulations are available to those planning interventions in traditional and historic buildings.



CONTENTS

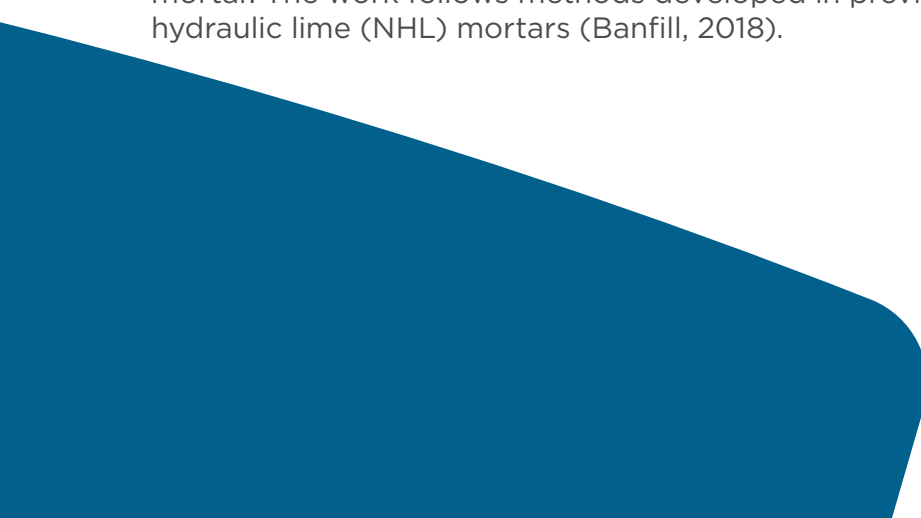
Author Biography	3
Preface	4
1 Introduction	6
2 Materials	7
2.1. Hot-mixed lime mortar	7
2.2. Earth mortar	8
2.3. Selected building stones	8
3 Procedures	9
3.1. Preparation of specimens	9
3.2. Testing	10
4 Results and Discussion	14
4.1. Initial comments on the Craigleith specimens	14
4.2. Confidence limits in the measured data	14
4.3. Water vapour permeability - dry cup method	15
4.4. Water vapour permeability - wet cup method	17
4.5. Thermal conductivity	20
4.6. Sorptivity and water absorption coefficient	21
4.7. Hygroscopic sorption	24
4.8. Density	29
4.9. Porosity	30
5 General Discussion	38
5.1. Veracity of the measured data	38
5.2. Application of the information to hygrothermal simulation	41
5.3. Limitations	42
6 Conclusion	44
7 Contacts	45
8 Bibliography	46
9 HES Technical Conservation Publication Series	48
Appendix: Tables of values for use in WUFI	49

I INTRODUCTION

Water can cause deterioration of a building's fabric and create unhealthy indoor environments. It is, therefore, a major factor of consideration in construction design and detailing. Water transport and heat transfer are interdependent, and their behaviour is described in hygrothermal building physics (Künzel, 1995). Traditional solid masonry walls breathe (i.e. they permit moisture vapour to pass from high humidity internal spaces to the lower humidity exterior) (Jenkins and Curtis, 2014; McCaig et al, 2018; Prince's Regeneration Trust, 2015). This moisture transfer ability is a major factor in determining the performance and durability of solid masonry construction. However, the drive to install more insulation in order to reduce energy consumption poses a risk of upsetting the equilibrium within a wall, because heat and moisture transport are coupled. In fact, energy efficiency retrofits to improve the thermal performance of the building fabric almost always change its moisture performance as well. Fortunately, hygrothermal building performance simulation software such as WUFI® (2020) offers the possibility of predicting the effect of a retrofit intervention at the design stage (Little et al, 2015).

The simulation software requires values for several physical properties of the materials that make up the fabric of the building under consideration – density, thermal conductivity, water vapour permeability or vapour diffusion resistance factor, specific heat capacity, water absorption coefficient, hygrothermal sorption and porosity – and WUFI provides a database of numerical values. However, there are no Scottish masonry materials in the database. A recent English report (MHCLG, 2019) giving technical guidance on the risk of moisture-induced damage in both new and retrofit construction confirms that “there is currently a lack of tested or standardised material characteristics for those typically used in the UK construction industry. In the absence of such data the material databases in WUFI are the best source of currently available data.”

Therefore, Historic Environment Scotland commissioned Heriot-Watt University to collect information on the hygrothermal properties of typical Scottish masonry materials. The work will contribute to a Scotland-specific data set of masonry properties which can be used by designers to ensure that retrofits meet the moisture-related needs of traditional buildings, as well as achieve energy efficiency. The objective of this paper is to determine the water vapour permeability, thermal conductivity, sorptivity/water absorption coefficient, hygroscopic sorption, density and porosity of a range of building stones, a hot-mixed lime mortar (in both the uncarbonated and carbonated states), and an earth mortar. The work follows methods developed in previous work on contemporary, natural hydraulic lime (NHL) mortars (Banfill, 2018).



2 MATERIALS

Except where specifically noted, all material samples were obtained between October 2018 and January 2019. A description of the materials and the preparation process is provided below, and the selected building stones included stones currently in production, as well as common historic building stones no longer quarried.

2.1. HOT-MIXED LIME MORTAR

By courtesy of Andrew Stockdale, resident mason, and Kate Darrah, Managing Director, approx. 20 litres of hot-lime mixed mortar were collected from an active work site at The Ridge Foundation, Black Bull Close, Dunbar. The mix proportions were (by volume) 1 part kibbled quicklime (Shap Limestone, Cumbria) : 2 parts concrete sand (Lothian Building Supplies, Dunbar) : 1 part building sand (Lothian Building Supplies, Dunbar). The sand particle size distributions, obtained by dry sieving, are shown in Figure 1. The mortar was prepared on site by placing water, followed by half of the concrete sand and all of the building sand, and finally the quicklime, in a 25-litre capacity electric mixer. It was mixed for about 5 minutes and then the remainder of the concrete sand added and further mixed for 5 minutes. The mixed mortar was then transported back to the laboratory at Heriot-Watt University and cast into the specimen moulds, as described below. The whole process was completed within 5 hours of mixing.

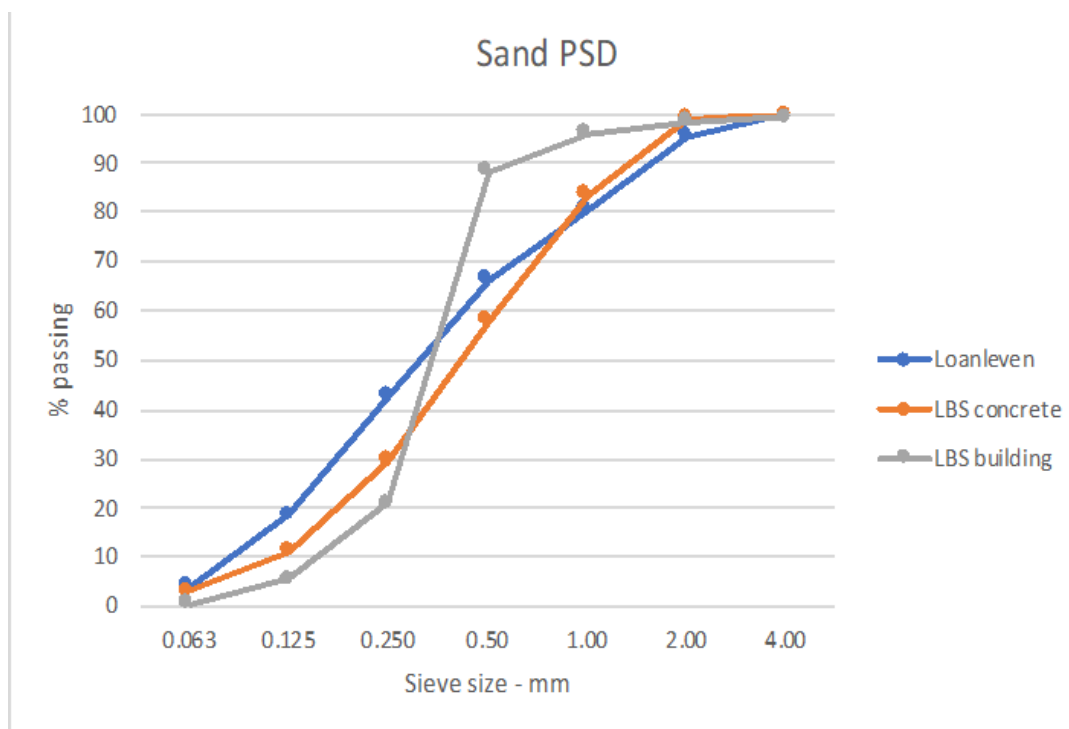


Figure 1 - Particle size distributions of the sands used in the mortars (LBS denotes Lothian Building Supplies).

2.2. EARTH MORTAR

By courtesy of Andrew Stockdale, resident mason, and Kate Darrah, Managing Director, approx. 20 kg of earth were collected from the active work site at The Ridge Foundation, Black Bull Close, Dunbar. This material was salvaged from walling (thought to date from the late 16th century) that had been demolished as part of the restoration work. It was transported back to the laboratory at Heriot-Watt University where some vegetable matter and coarse particles of stone were removed. Mortar consisting of 1 part earth : 2 parts Loanleven concrete sand (particle size distribution shown in Fig. 1) was mixed in a Hobart bench-top mixer for 5 minutes, adding water to obtain a similar consistency to that of the hot-mixed lime mortar, and cast into specimen moulds, as described below.

2.3. SELECTED BUILDING STONES

(i) Current production

- Hazeldean sandstone, Alnwick, Northumberland, was taken from a stock obtained in 2015 from Hutton Stone, Berwick-upon-Tweed.
- Locharbriggs sandstone, Dumfries and Galloway, was obtained by courtesy of Cumbria Quarrying Services, Bowscar Quarry, Penrith.
- Scottish Whinstone, West Lothian, was purchased (cut to our size requirements) from Tradstocks Ltd, Thornhill, Stirlingshire.

(ii) Production now ceased

- Rubislaw granite was widely used in Aberdeen but is no longer available. Crathes granodiorite is a close geological match and was until recently worked for roadstone. Several irregular shaped lumps (about 10 kg each) were obtained in 2015 from Craigenlow Quarry, Aberdeenshire.
- Craigleith sandstone was widely used in Edinburgh, including the building of Old College, but is no longer available. Two samples of stone removed during conservation works at Old College, Edinburgh, were obtained by courtesy of Gary Jebb, Director of Estates, Edinburgh University. Craigleith A was taken from the external face and Craigleith B from the inside of an external wall. As described below, Craigleith B could equally well have been sourced from the “feak” rock of the Craigleith Quarry as from Hailes Quarry, which produced an essentially indistinguishable bedded sandstone, which was widely used in Edinburgh.
- Giffnock sandstone was widely used in Glasgow and Belfast but is no longer available. Samples of stone removed during conservation works at The Lanyon Building, Queens University, Belfast, were obtained by courtesy of Joanne Curran, Consarc Architects. Some surface weathering was visible.

3 PROCEDURES

3.1. PREPARATION OF SPECIMENS

The hot-mixed lime mortar was cast into six 100mm cubes, using lightly oiled steel moulds, and three 360 × 240 × 10±1mm thick tiles, using timber moulds lined with cling film to ensure easy demoulding. The moulds were filled by hand tamping, followed by the minimum of hand trowelling to ensure a smooth finish. While the mortar was fresh the tiles were scored through with the point of a trowel to provide twenty 90 × 120 rectangular zones. The specimens and moulds were covered with cling film and placed in a high humidity environment for 17 days and then demoulded. By this time, the material was firm enough to be handled with care and the scoring process enabled the tiles to be separated gently into 90mm × 120mm tiles. All specimens were then placed (moist) in airtight containers for a further four weeks, whereupon half were placed in a TAS3 environmental controlled chamber at 20°C, 60% RH and 600ppm CO₂. These conditions had previously been successfully used to produce fully carbonated lime mortars. The other half of the cubes and tiles were left in the airtight containers to remain uncarbonated until required for testing. Being fragile, some tiles broke during handling, so it was not always possible to produce the intended ten 90mm x 120mm tiles for testing in both the uncarbonated and carbonated state and these circumstances are noted in the results presented below.

The earth mortar was similarly cast into three 100mm cubes, using lightly oiled steel moulds, and two 360mm × 240mm × 12±1mm thick tiles, using timber moulds lined with cling film. They were hand tamped and finished with a minimum of hand trowelling, and tiles scored through as above. The compacted mortar was firm enough to be demoulded from the cube moulds immediately and placed on a non-absorbent plate in the TAS3 chamber. The tiles were left in the cling film-lined moulds, and all were placed in the chamber at 20°C, 60% RH and 600ppm CO₂. The tiles were demoulded after 7 days. All specimens were maintained in these conditions until testing.

The building stone samples were cut with a bench-mounted circular saw (Norton Clipper CM501) using a water-cooled diamond tipped blade. Because of the irregular shape of some of the samples, it was not always possible to produce the intended three 100mm cubes and ten 90 × 120 × 12±3mm tiles and these are noted in the results presented below. Any surface weathering was carefully excluded from the prepared specimens. The Crathes granodiorite was too hard for this saw and the requisite specimens were cut for us by courtesy of Stirling Stone Ltd. The Scottish whinstone was supplied cut to size by Tradstocks. Figure 2 shows the surface appearance of the prepared stone tiles.

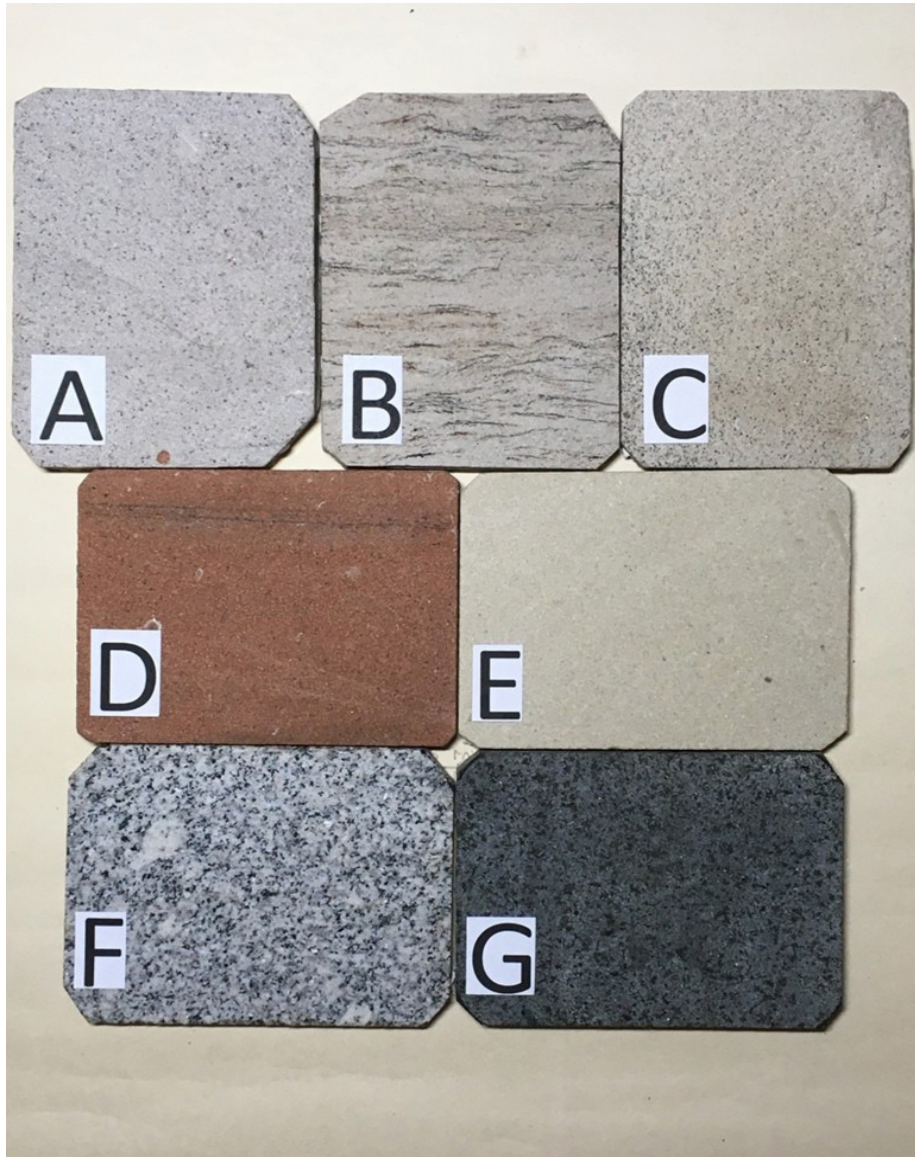


Figure 2 - Cut surfaces of the 90 x 120mm prepared stone specimens (Key: A - Craigleith A, B - Craigleith B, C - Giffnock, D - Locharbriggs, E - Hazeldean, F - Granodiorite, G - Scottish whinstone).

3.2. TESTING

(i) Water vapour permeability

The water vapour permeability was determined by both dry cup and wet cup methods according to BS EN ISO 12572:2001 (BSI, 2001).¹ After curing/carbonating or cutting to size as described above, the tiles were conditioned to 50% RH and their thicknesses measured with a digital calliper in four places, and the mean value used in calculating the results. That the relevant lime mortar specimens were either fully carbonated or uncarbonated was confirmed by spraying an alcoholic solution of phenolphthalein indicator onto a freshly fractured surface of dummy tiles kept alongside the test tiles. For

¹ The notes in this standard (BSI, 2001) explain that dry cup tests give information about the performance of materials at low humidities where moisture transfer is dominated by vapour diffusion. Wet cup tests give guidance about the performance of materials under high humidity conditions. At higher humidities the pores in the material start to fill with water, which increases the transport of liquid water and reduces the transport of water vapour.

the dry cup test, up to five tiles were sealed into aluminium foil cups (General Stores Ltd) containing dry calcium chloride desiccant (Vida XL, UK). For the wet cup test, up to five tiles were sealed into cups containing a saturated solution of potassium nitrate (Akros Organics, Belgium) to provide an internal atmosphere at 93% RH. Having first trimmed any irregularities in the perimeter, tiles were placed (mortars with the cast face up) onto a narrow bead of silicone sealant (Unibond plc, UK) to create an air- and liquid-tight seal, as shown in Figures 3 and 4. The cut stone tiles were randomly oriented on the foil cups because it was impossible to exert control over the angle of cutting related to bedding planes. The face area of specimens exposed to the dry or humid environment in the foil cups achieved by this procedure was 9396mm². The residual gap between the perimeter and the wall of the cup was sealed using molten paraffin wax (Akros Organics, Belgium). The assembled tiles/cups were then placed in the TAS3 environment chamber at 23°C and 50% RH and removed and weighed (to ±0.01g) at intervals over several weeks, taking care to record each time of weighing to within ±10 minutes.

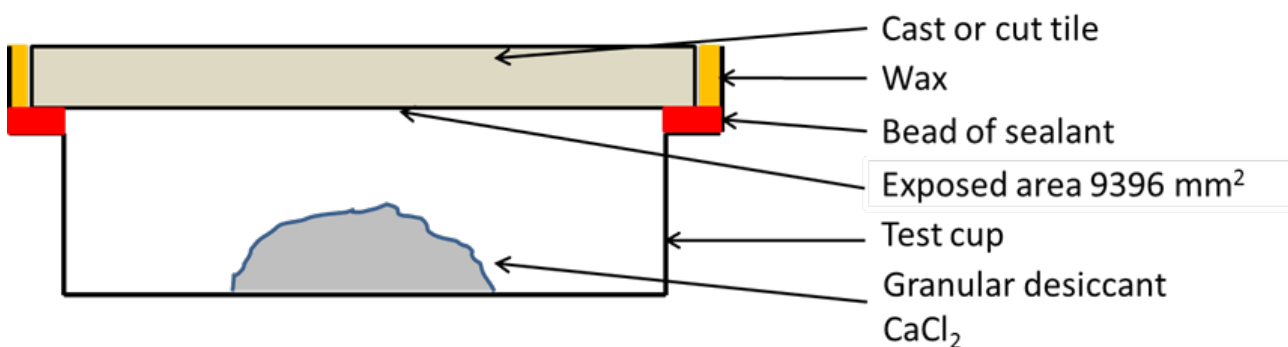


Figure 3 - Dry cup test apparatus.

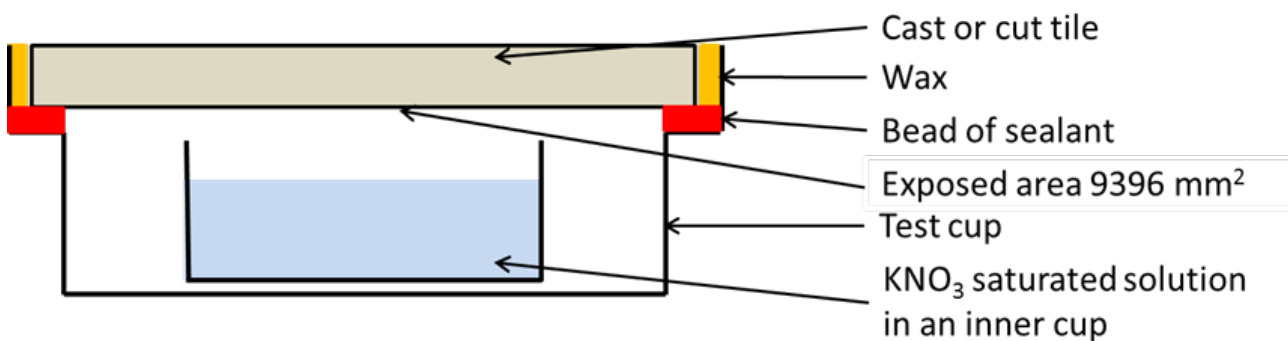


Figure 4 - Final version of wet cup apparatus.

The thermal conductivity was determined in both the dry and saturated conditions using the Thermtest TLS-100 instrument (Thermtest inc, Fredericton, Canada) and the thermal probe method to ASTM D5334-14 (ASTM, 2014). For this test, the 100mm square cubes of the materials were used. The stone samples were dried to constant mass at 105°C and the lime and clay mortar samples were dried to constant mass at 50°C, and a 3mm groove was cut on one face of each specimen using a stone cutting disc mounted in a handheld angle grinder. The probe was placed in the groove, surrounded by thermal contact paste (thermal conductivity 5W/(m K), RS Components, UK, Fig. 5) and covered with a second specimen of the same material. This ensured that the required test

condition of a minimum of 25mm thickness of material around the probe was met. The test was replicated on three specimens of each material. In the test, the probe is heated and the temperature decay over time is measured accurate to 0.001°C. The internal software calculates the thermal conductivity of the material surrounding the probe. The test was repeated after the specimens had been immersed for a week in water at room temperature.



Figure 5 - Thermtest TLS-100 thermal conductivity probe located in a groove in the face of a specimen.

(iii) Sorptivity and water absorption coefficient

Water sorptivity and water absorption coefficient were determined gravimetrically by immersing one face (measured to $\pm 1\text{mm}$) of each prepared specimen in water to a depth of 2mm and weighing at intervals over 2-3 hours or until water was visible on the top face, according to BS EN ISO 15148:2002 (BSI, 2002). The test was replicated on three specimens of each material. The earth mortar was not tested because it disintegrated in contact with water.

(iv) Hygroscopic sorption

The moisture absorption and desorption curves were determined according to BS EN ISO 12571:2013 (BSI, 2013). Fragments of each material, weighing 20-50g, were oven dried to constant mass, then placed successively in airtight boxes supported in the atmosphere over saturated salt solutions, giving nominal relative humidities (RH) of 33% (MgCl_2), 53% ($\text{Mg}(\text{NO}_3)_2$), 75% (NaCl), 85% (KCl) and 93% (KNO_3), and water (100% RH). The RH was tested, and the fragments removed for weighing at intervals until constant mass was achieved (up to 7 days). The absorption curves were determined at successively increasing RH, after which the desorption curves were obtained at successively decreasing RH, until a final oven dried mass gave a confirmation value. The test was replicated on three fragments of each material.

(v) Density

The density of each material was determined by displacement of water. Three replicate specimens, saturated after completion of the sorptivity test, were suspended beneath a balance and then weighed both in air and when immersed in water. The specimens were then oven dried to constant mass and the test repeated. When immersed in water, care was taken to complete the weighing quickly before significant absorption had occurred. The earth mortar cubes were wrapped in cling film to prevent disintegration on contact with water. The temperature of the water, measured at the time of testing, was used to determine the density of the water used in the calculation (Kaye and Laby, 1966).

(vi) Porosity

Samples of each material were submitted to the University of Dundee, where porosity and pore size distribution were determined by mercury intrusion using a Quantachrome PoreMaster33 instrument, and a sample cell of diameter 8mm × 20mm and capillary volume of 0.5ml, with 33000 psi final pressure, on a single fragment of each material of mass approximately 2g.

4 RESULTS AND DISCUSSION

4.1. INITIAL COMMENTS ON THE CRAIGLEITH SPECIMENS

When the Craigleith samples from Old College were cut into the required specimens, A and B looked sufficiently different to raise the question of whether they were in fact different stones. Weathering and applied finishes had concealed this, and the results presented below are consistently different. Craigleith A is uniformly cream coloured whereas Craigleith B is greyer with frequent dark wispy laminar banding. Therefore, samples of each stone were submitted to the Scottish Lime Centre Trust for petrographic analysis of thin sections in order to identify the two stones with confidence. Their report (SLCT, 2019) concludes that Craigleith A is “most likely” Craigleith stone. However, Craigleith B may equally well have come from two sources. Firstly, it could be the “feak” rock of Craigleith Quarry, which is a ripple bedded sandstone recorded as having been used for rubble work, foundations, steps and paving. Secondly, and equally likely, it could be from Hailes Quarry, which produced an essentially indistinguishable bedded sandstone, widely used in Edinburgh.

4.2. CONFIDENCE LIMITS IN THE MEASURED DATA

In all the tests except for porosity, several replicate specimens were measured to give an estimate of experimental variability and, therefore, confidence limits which are applicable to the data. This section briefly describes the principle behind the assessment of error.

Following the well-established statistical principles of the design and analysis of experiments (Davies, 1957; Chatfield, 1970), the measurements could be evaluated by a one-way Analysis of Variance (ANOVA). In the ANOVA, the overall variation is considered to be the sum of the “explained” variation due to the differences between materials and the “residual” variation due to differences in specimen preparation and handling, plus the experimental error. According to Chatfield (1970), the residual is an estimate of the variance σ^2 in the population of measurements. Because significant differences between the mean values of each property are to be expected for the different materials, it is only necessary to use the ANOVA procedure to estimate the residual, and this was done as follows. If $x_{1j}, x_{2j} \dots x_{ij}$ are the measured values of a property x for the i th test on material j , a total sum of squares tss can be calculated as:

$$tss = \sum_{i=1}^c \sum_{j=1}^n (x_{ij} - \bar{x}_j)^2$$

where c is the number of replicate tests and n is the number of materials. Dividing this by the number of degrees of freedom (df) gives the mean square as $tss/(n(c-1))$ and the square root of this mean square gives an estimate of the standard error σ . The latter can be multiplied by the appropriate value of the t-distribution to give the confidence interval. As an example, for the density measurements (see below), 10 materials were tested dry and 9 tested saturated, so $n = 19$ and $c = 3$, giving 38 df. Statistical tables (Chatfield, 1970) give the 5% point of the Student’s t-distribution for 38 df as $t_{0.05} = 1.685$

from which the 90% confidence interval is $\pm 1.685 \times \sigma$. In situations where the measured values cover a very wide range, such as the sorptivity and water absorption coefficient, a fixed confidence interval is inappropriate, and a base-10 logarithmic transformation was applied to the raw data. In this case, the standard error and confidence interval are equivalent to a fixed percentage of the mean value.

This procedure was applied to all the replicated measurements and the resulting confidence intervals and numbers of replicates contributing to each mean are all shown in the tables below. The confidence intervals estimated in this way are an indication of the variation between individual specimens of materials, manufactured or obtained at the same time from the same source for the purposes of this investigation, combined with the measurement error.

4.3. WATER VAPOUR PERMEABILITY – DRY CUP METHOD

Figure 6 shows an example of the raw data collected from the weighings of the complete foil tray/tile specimen assembly. BS EN ISO 12572:2001 (BSI, 2001) requires the increments of mass over five successive measurement intervals (i.e. six points) to be constant within 5% of the overall average rate of mass gain. This corresponds to a value of $R^2 = 0.9998$ ($R^2 = 1.0$ corresponds to a perfect straight line) and was achieved by only one assembly out of the 31 that gave six points. However, 16 achieved $R^2 > 0.9990$ and the lowest value was $R^2 = 0.9964$ (Fig. 6). At most, six measurement points were obtained at weekly intervals, but the more permeable materials reached saturation of the CaCl_2 desiccant in this time. When this happened, the saturated CaCl_2 solution in the bottom of the aluminium foil trays unfortunately crept, by capillary attraction, up the crinkles present in the corners of the trays. This wetted the specimens and either evaporated from the surface to leave crystal deposits behind or dripped back from the lip of the tray. In either case, the mass loss is not just due to permeation of water vapour through the tile and, therefore, the calculated permeability is over-estimated. Accordingly, weighings were terminated on assemblies where this happened and, as a result, some materials have fewer measurement points. This accounts for the lower values of R^2 observed in these tests. Nevertheless, all assemblies showed a linear increase in mass, driven by the vapour pressure difference between the TAS chamber environment at 23°C and 50% RH and the internal 0% RH environment within the assembly. The slope of the line gives the water vapour flow rate, from which the water vapour permeability is given by the relationship:

Permeability = (slope × specimen thickness) / (exposed area × vapour pressure difference).

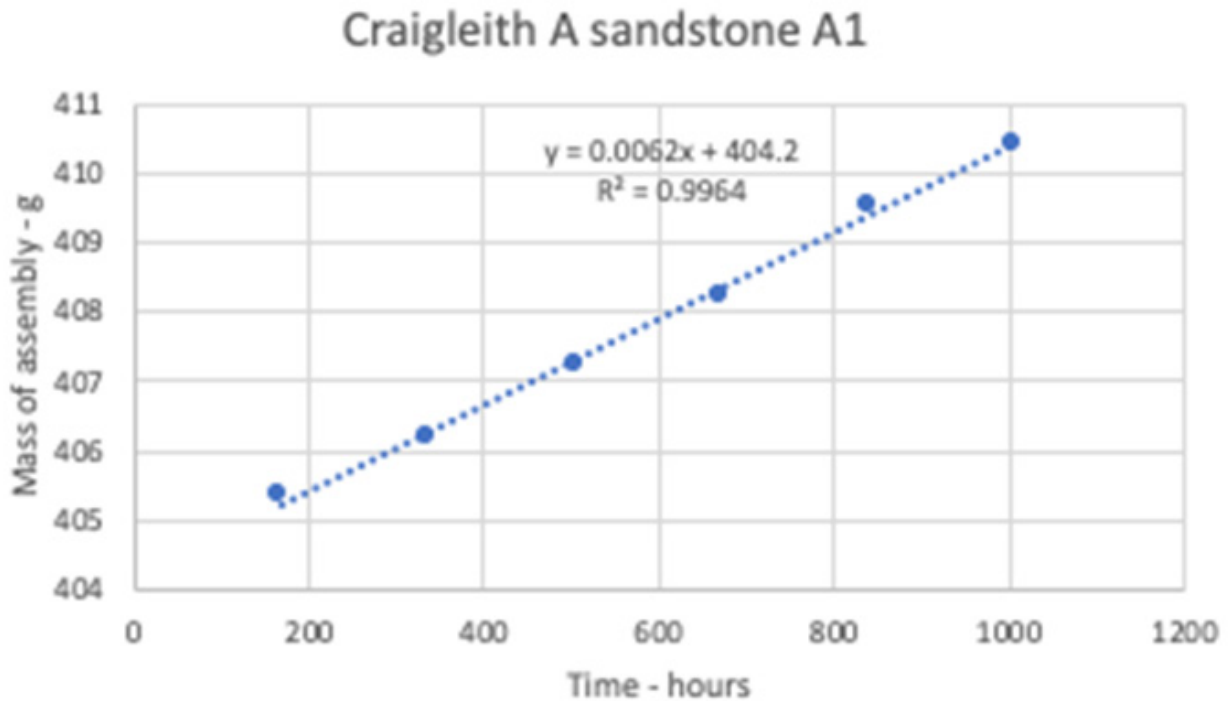


Figure 6 - Variation in mass of assembly for Craigleith A specimen A1 in the dry cup test.

WUFI software requires values of the vapour diffusion resistance factor, defined as the water vapour permeability of air divided by that of the material. This indicates how much greater the resistance of the material is compared to an equally thick layer of still air at the same temperature. The water vapour permeability of air at 23°C and 1000 mbar atmospheric pressure is given as 1.8×10^{-10} kg/(m sec Pa) (BSI, 2001). Table 1 summarises the water vapour permeability and vapour diffusion resistance factor for each material, calculated in this way, together with an estimate of the confidence intervals associated with each value.

For consideration of the experimental error, the materials were divided into two groups - (i) Scottish whinstone and Crathes granodiorite in a low permeability group (8 df) and (ii) all the others in a higher permeability group (29 df). For group (i) the standard error is 0.34×10^{-12} , corresponding to a confidence interval of about $\pm 0.6 \times 10^{-12}$ kg/(m sec Pa), and for group (ii) this is 0.05×10^{-12} , corresponding to a confidence interval of about $\pm 0.09 \times 10^{-12}$ kg/(m sec Pa). Because of the inverse relationship between water vapour permeability and vapour diffusion resistance factor, the confidence interval for the latter has been calculated from the values of vapour diffusion resistance factor corresponding to the upper and lower limits of water vapour permeability. This can be shown by the example of earth mortar. Taking its mean water vapour permeability (Table 1) as 6.23 (units of 10^{-12} kg/(m sec Pa)) the upper and lower confidence limits are 6.83 and 5.63 respectively. The corresponding values of vapour diffusion resistance factor are 26.35 and 31.97, giving a confidence range of 5.6 centred on 29.16, which is reported in the table as 29 ± 3 . This explains why the confidence limits for vapour diffusion resistance factor given in Table 1 are not the same for every material.

Table 1 - Water vapour permeability values (means of 5 specimens except for those tests marked * which are means of 4), using dry cup tests.

Material	Water vapour permeability (10^{-12} kg/(m sec Pa))	Vapour diffusion resistance factor
Uncarbonated lime mortar	7.85±0.6*	23±2
Carbonated lime mortar	7.84±0.6*	23±2
Earth mortar	6.23±0.6	29±3
Hazeldean sandstone	4.90±0.6	37±5
Locharbriggs sandstone	6.07±0.6	30±3
Craigleith A	1.50±0.6	120±50
Craigleith B	2.84±0.6	63±15
Giffnock sandstone	4.90±0.6*	37±5
Scottish whinstone	0.13±0.09	2200±1500
Crathes granodiorite	0.17±0.09	1050±500

From this analysis, the following features emerge. The water vapour permeability covers a 60-fold range and is highest for the mortars, reflecting their high porosity and open texture, and lowest for the very dense whinstone and granodiorite, whose permeability is less than 10% that of the lowest sandstone. The lime mortars are indistinguishable; the Locharbriggs sandstone and the earth mortar are indistinguishable; Hazeldean and Giffnock are identical; and Craigleith somewhat lower. Using the confidence intervals above, the materials may be grouped in the following order: lime mortar > earth mortar, Locharbriggs sandstone > Giffnock, Hazeldean sandstones > Craigleith B > Craigleith A > Crathes granodiorite, Scottish whinstone.

4.4. WATER VAPOUR PERMEABILITY – WET CUP METHOD

The first set of wet cup tests were beset by experimental difficulties. First, it was found that similarly to the CaCl_2 in the dry cup test, the saturated KNO_3 solution in the bottom of the aluminium foil trays crept, by capillary attraction, up the crinkles present in the corners of the trays. By 24 hours, this had wetted the specimens and started evaporating from the surface to leave crystal deposits behind. This problem was resolved by dismantling everything, placing the saturated KNO_3 solution in a separate cup, as shown in Figure 4, and re-assembling every specimen/tray combination. Second, further contamination problems occurred by capillary creep of the now-saturated CaCl_2 solution in high permeability dry cup specimens on higher shelves of the TAS chamber, leading to solution dripping on to wet cup specimens on the lower shelves. Finally, the humidity control in the chamber failed, terminating the experiment after four measurements at most. Following an extended period of time, during which the service engineers

visited the laboratory to replace various components and make adjustments without success, a new series of tests were set up in a WKL100 controlled humidity chamber (Weiss Instruments, Germany) at 23°C and 50% RH. In order to fit in with other work using this chamber, a maximum of 9 weighings were possible over a 16-day period. This had implications for the precision of the results for the two materials with very low permeability - Crathes granodiorite and Scottish whinstone - as will be discussed later.

All assemblies showed a linear decrease in mass, driven by the vapour pressure difference between the WKL100 controlled environment at 23°C and 50% RH and the internal 93% RH environment within the assembly. Figure 7 shows the raw data for the foil/cup assembly that displayed the lowest value of R^2 for the 9 measurement points for the higher permeability group of materials: the highest value of R^2 was 1.0. For Crathes granodiorite and Scottish whinstone, the total decrease in mass was about 0.5g, which means that experimental errors are relatively large leading to low values of R^2 . Figure 8 shows the raw data for the foil/cup assembly that showed the lowest value of R^2 for the 9 measurement points for the low permeability materials: even so, the highest value of R^2 was 0.9984. As before, the slope of the line gives the water vapour flow rate from which the water vapour permeability is given by the formula:

Permeability = (slope x specimen thickness) / (exposed area x vapour pressure difference)

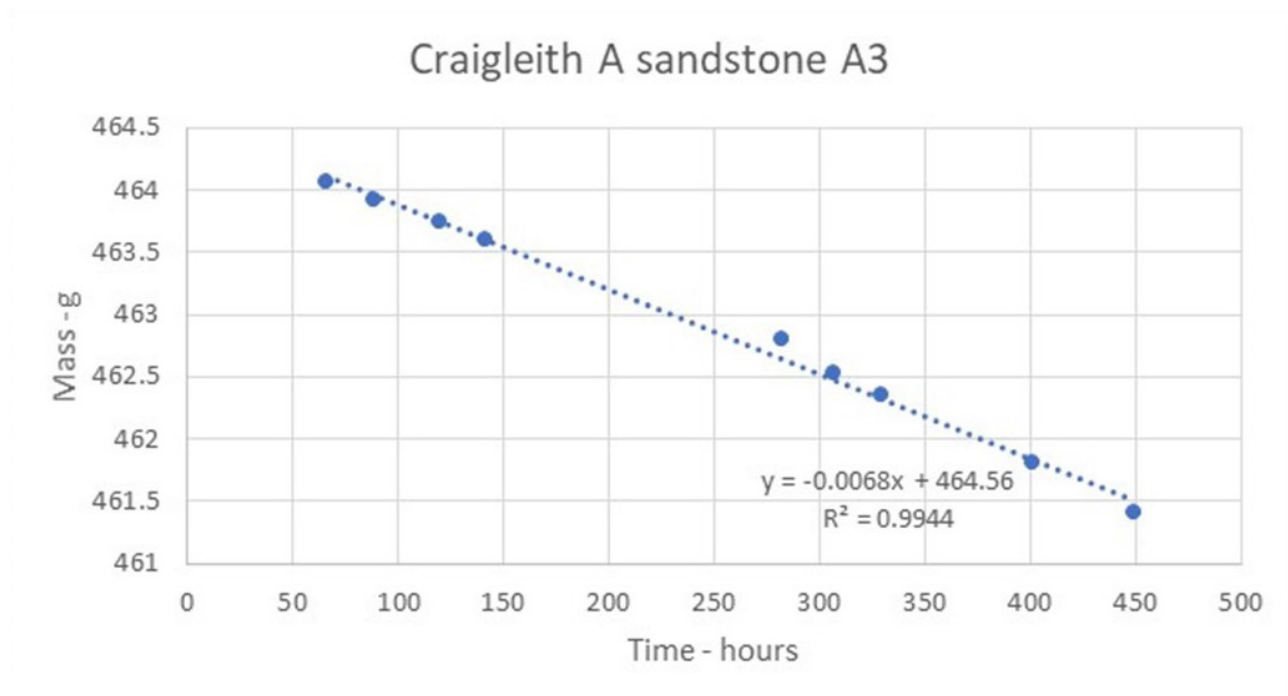


Figure 7 - Variation in mass of assembly for Craigleith A specimen A3 in the wet cup test.

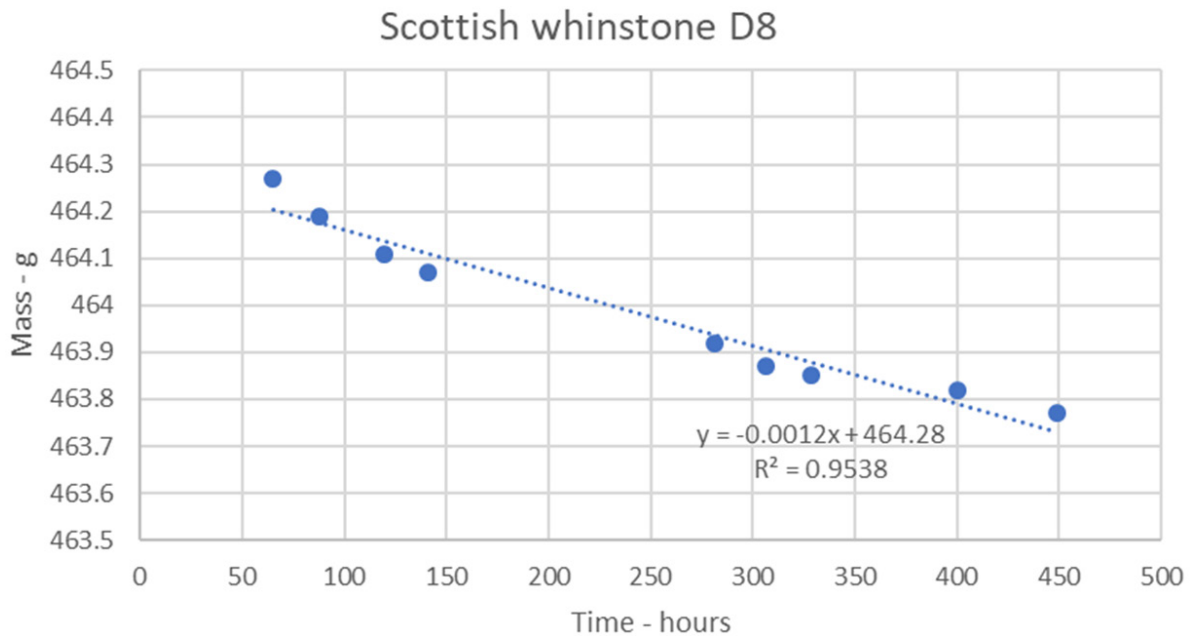


Figure 8 - Variation in mass of assembly for Scottish whinstone specimen D8 in the wet cup test.

Table 2 summarises the water vapour permeability and the vapour diffusion resistance factor for each material, calculated in the same way as for the dry cup tests. As before, for consideration of the experimental error associated with the values of water vapour permeability, the materials were divided into two groups. For group (i) the standard error (8 df) is 0.057×10^{-12} , corresponding to a confidence interval of about $\pm 0.1 \times 10^{-12}$ kg/(m sec Pa), and for group (ii) the standard error (28 df) is 1.205×10^{-12} , corresponding to a confidence interval of about $\pm 2.2 \times 10^{-12}$ kg/(m sec Pa). The confidence intervals for the vapour diffusion resistance factor were calculated from the water vapour permeability at the upper and lower confidence limits and range from ± 2.5 for the mortars to ± 200 for the whinstone. These confidence intervals are larger than for the dry cup tests, reflecting wider variations among the measured permeability for different samples of each material, but allow the following features to emerge.

Table 2 - Water vapour permeability values (means of 5 tests except for those marked * which are means of 4 and that marked ** which is mean of 3), using wet cup tests.

Material	Water vapour permeability (10 ⁻¹² kg/(m sec Pa))	Vapour diffusion resistance factor
Uncarbonated lime mortar	12.94±2.2*	14±2.5
Carbonated lime mortar	13.54±2.2	13±2.5
Earth mortar	14.73±2.2*	12±2
Hazeldean sandstone	8.01±2.2	22±7
Locharbriggs sandstone	10.47±2.2	17±4

Craigleith A	2.86±2.2**	63±50
Craigleith B	6.64±2.2	27±10
Giffnock sandstone	10.09±2.2	18±4
Scottish whinstone	0.31±0.1	580±200
Crathes granodiorite	0.36±0.1	500±150

First, all materials show higher water vapour permeability in the wet cup tests than in the dry cup. The difference, a factor of 1.6-2.4, is well known and is attributed to condensation in the pores at the higher RH in the test. Second, the wet cup permeability covers a nearly 50-fold range and is highest for the mortars, reflecting their high porosity and open texture, and lowest for the very dense whinstone and granodiorite. Using the confidence intervals above, the materials may be grouped in the following order: lime mortar, earth mortar > Locharbriggs, Giffnock, Hazeldean sandstones > Craigleith B > Craigleith A > Crathes granodiorite, Scottish whinstone.

4.5. THERMAL CONDUCTIVITY

Table 3 summarises the thermal conductivity and confidence interval for each material in the oven-dry and saturated conditions, together with the moisture content (by mass) at saturation. The earth mortar specimens disintegrated on contact with water, so the saturated thermal conductivity and the moisture content at saturation was not determined.

For consideration of the experimental error, the materials were divided into two groups, same as for the permeability. In this case, group (i), the mortars (10 df), gave a standard error of 0.19, corresponding to a confidence interval of about ±0.35 W/(m K), and for group (ii), the stones (28 df), the standard error is 0.597 W/(m K), corresponding to a confidence interval of about ±1.0 W/(m K).

Table 3 - Thermal conductivity values oven-dry and saturated (means of 3 specimens).

Material	Thermal conductivity (dry) (W/(m K))	Thermal conductivity (saturated) (W/(m K))	Moisture content at saturation %w/w
Uncarbonated lime mortar	0.22±0.35	0.83±0.35	18.40
Carbonated lime mortar	0.20±0.35	0.66±0.35	15.53
Earth mortar	0.22±0.35	-	-
Hazeldean sandstone	1.73±1	3.97±1	4.19
Locharbriggs sandstone	1.45±1	3.36±1	6.07

Craigleith A	1.71±1	4.28±1	1.82
Craigleith B	1.94±1	5.65±1	3.89
Giffnock sandstone	1.07±1	4.15±1	5.40
Scottish whinstone	1.43±1	2.41±1	0.21
Crathes granodiorite	2.13±1	2.77±1	0.21

From this analysis, the following features emerge. The thermal conductivity of the mortars is significantly lower than the stones, due to their lower density and higher porosity, as confirmed by their higher moisture content at saturation. Using the confidence intervals above, the dry materials fall into two groups, the mortars and the stones, and within the groups the differences are all within experimental error. The thermal conductivity of all the materials is significantly higher at saturation than in the oven dry condition, as would be expected, because the pores are filled with water instead of air/vapour. Again, the mortars form one group and the stones another, although Craigleith B appears to have a significantly higher thermal conductivity than all the other samples. The ratio of thermal conductivity (saturated) / thermal conductivity (dry) is highest for the most absorbent mortars and lowest for the least absorbent granodiorite and whinstone, again as expected from the amounts of water absorbed. However, this effect is less clearly marked for the other stones, suggesting that other factors, such as the connectivity of the pores, may play a part.

4.6. SORPTIVITY AND WATER ABSORPTION COEFFICIENT

The sorptivity and water absorption coefficient were determined for each specimen from the slope of the graph of mass increase against $\sqrt{\text{time}}$, divided by the area in contact with the water, measured to the nearest mm^2 . Figure 9 and 10 show a typical set of measured data for a material of low and high sorptivity respectively, exemplifying the linear relationship. Generally, the graphs for materials with low sorptivity showed more scatter with lower values of R^2 . In some cases, the later points fell below the line because the waterfront reached the free top surface of the specimen and no further mass gain could take place. These were excluded. Table 4 summarises the sorptivity and water absorption coefficient with confidence limits for each material. Earth mortar was not tested because it disintegrated in water.

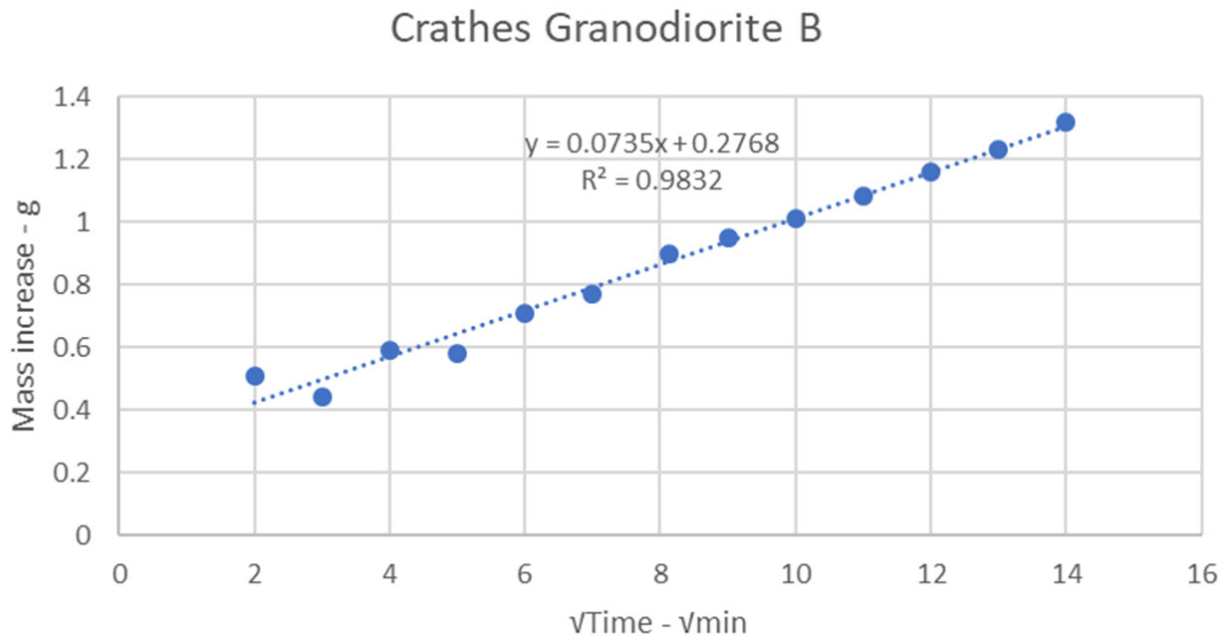


Figure 9 - Variation in mass of Crathes granodiorite specimen B under absorption.

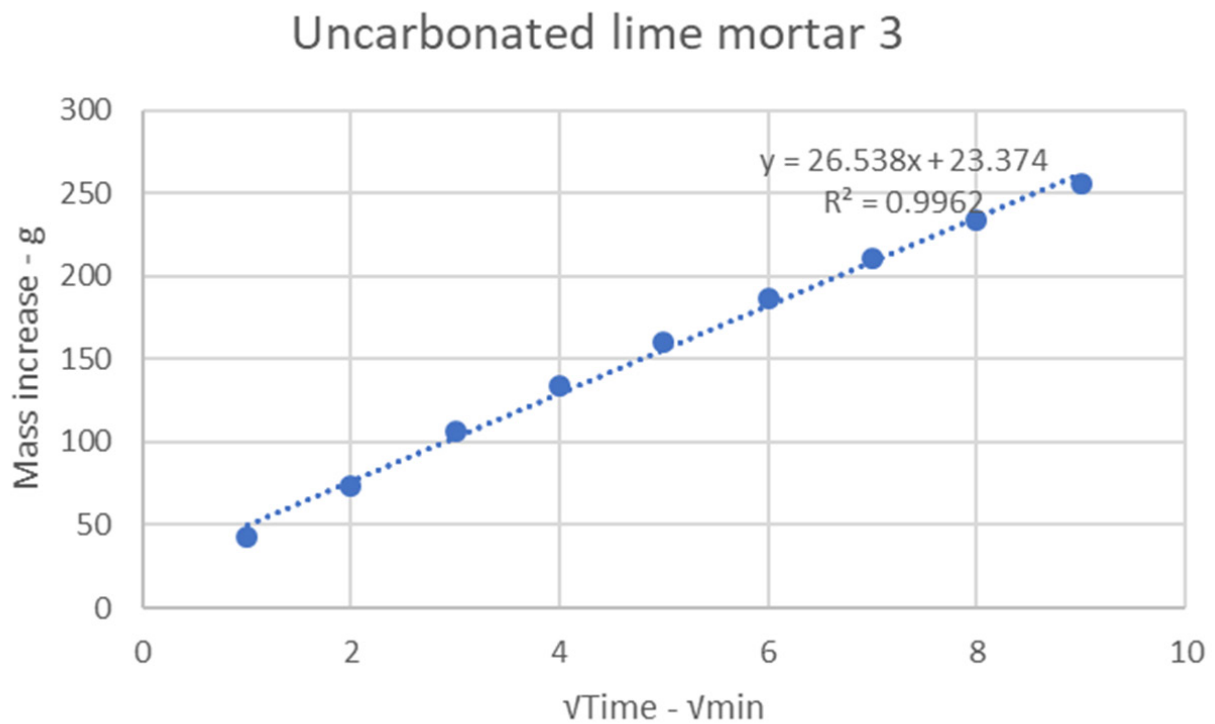


Figure 10 - Variation in mass of uncarbonated lime mortar specimen 3 under absorption.

For a consideration of the experimental error, the range of measured values precludes assigning the same confidence limits to each group of three replicates. Therefore, the measured values were transformed to their base-10 logarithm. This allows the standard error in log(sorptivity) and log(water absorption coefficient) to be estimated based on 18 df. The standard error in log(sorptivity) is 0.089, corresponding to a 90% confidence interval of about ± 0.15 in both log(sorptivity) and log(water absorption coefficient). Converting this result back to real numbers leads to an estimate of the confidence interval in each result as $\pm 41\%$, because:

$$\text{antilog}(\log x + \log 0.15) = x \times 1.41$$

Table 4 therefore shows a different confidence interval for each material in units of sorptivity and water absorption coefficient.

Table 4 - Sorptivity and water absorption coefficient of materials (means of 3 specimens).

Material	Sorptivity (mm/ $\sqrt{\text{min}}$)	Water absorption coefficient (kg/(m ² $\sqrt{\text{s}}$))
Uncarbonated lime mortar	2.15 \pm 0.9	0.28 \pm 0.11
Carbonated lime mortar	2.79 \pm 1.1	0.36 \pm 0.14
Earth mortar	-	-
Hazeldean sandstone	0.82 \pm 0.3	0.11 \pm 0.045
Locharbriggs sandstone	0.67 \pm 0.3	0.086 \pm 0.035
Craigeith A	0.063 \pm 0.025	8.14 $\times 10^{-3}$ \pm 3.2 $\times 10^{-3}$
Craigeith B	0.28 \pm 0.11	0.036 \pm 0.014
Giffnock sandstone	0.57 \pm 0.2	0.073 \pm 0.03
Scottish whinstone	0.0017 \pm 0.0007	0.22 $\times 10^{-3}$ \pm 0.09 $\times 10^{-3}$
Crathes granodiorite	0.0085 \pm 0.0035	1.1 $\times 10^{-3}$ \pm 0.44 $\times 10^{-3}$

The sorptivity and water absorption coefficient cover a 1600-fold range and are highest for the mortars, reflecting their high porosity and open texture, and lowest for the very dense whinstone and granodiorite, whose sorptivity is less than 10% that of the lowest sandstone. The lime mortars are indistinguishable, the Locharbriggs, Hazeldean and Giffnock sandstones are significantly lower, and Craigeith B somewhat lower again. Craigeith A is the lowest of all the sandstones. Using the confidence intervals above, the materials may be grouped in the following order: lime mortar > Hazeldean, Locharbriggs, Giffnock sandstones > Craigeith B > Craigeith A > Scottish whinstone, Crathes granodiorite.

4.7. HYGROSCOPIC SORPTION

Figures 11-19 show the sorption-desorption behaviour for each material as graphs of moisture content by mass (each point is the mean of the values for 3 specimens) against RH. In every case, there is some hysteresis and the moisture content on the downcurve is higher than that on the upcurve: i.e. more moisture is retained in the material as the RH to which it is exposed decreases. The results for Scottish whinstone are excluded because they make no sense: the moisture content apparently reached by water vapour sorption was several times that reached by liquid saturation. This suggests an experimental problem, probably specimen contamination.

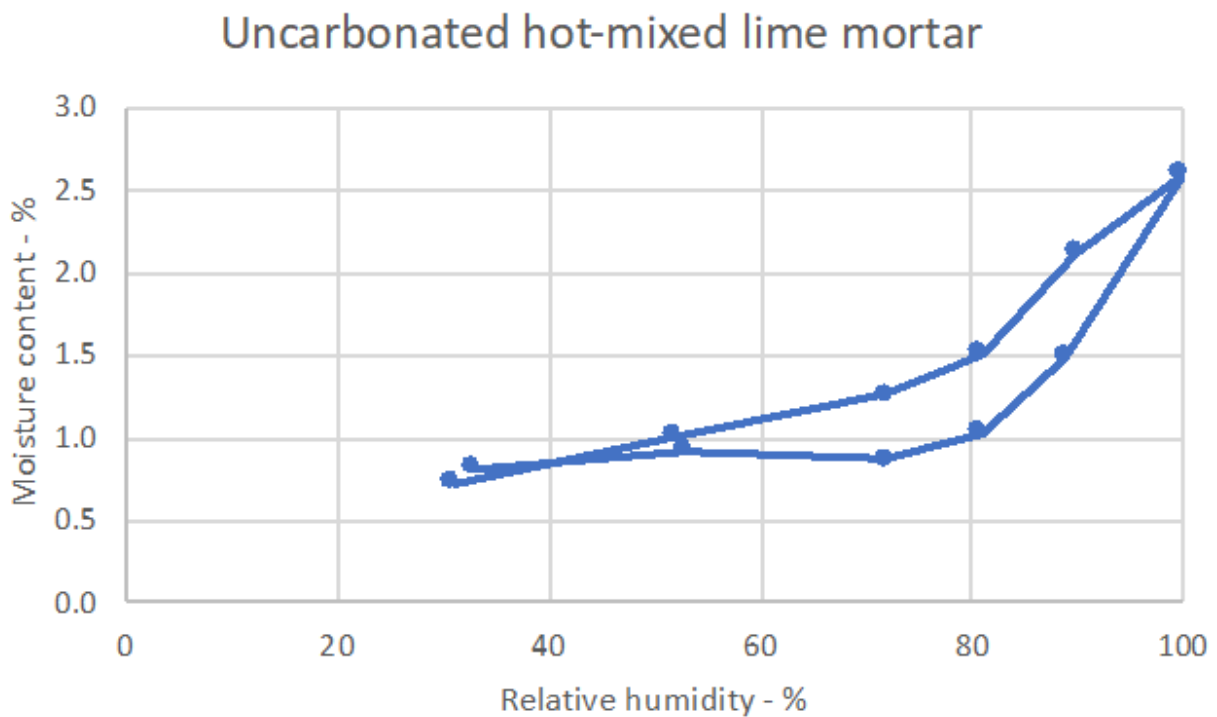


Figure 11 - Sorption-desorption curves for uncarbonated lime mortar.

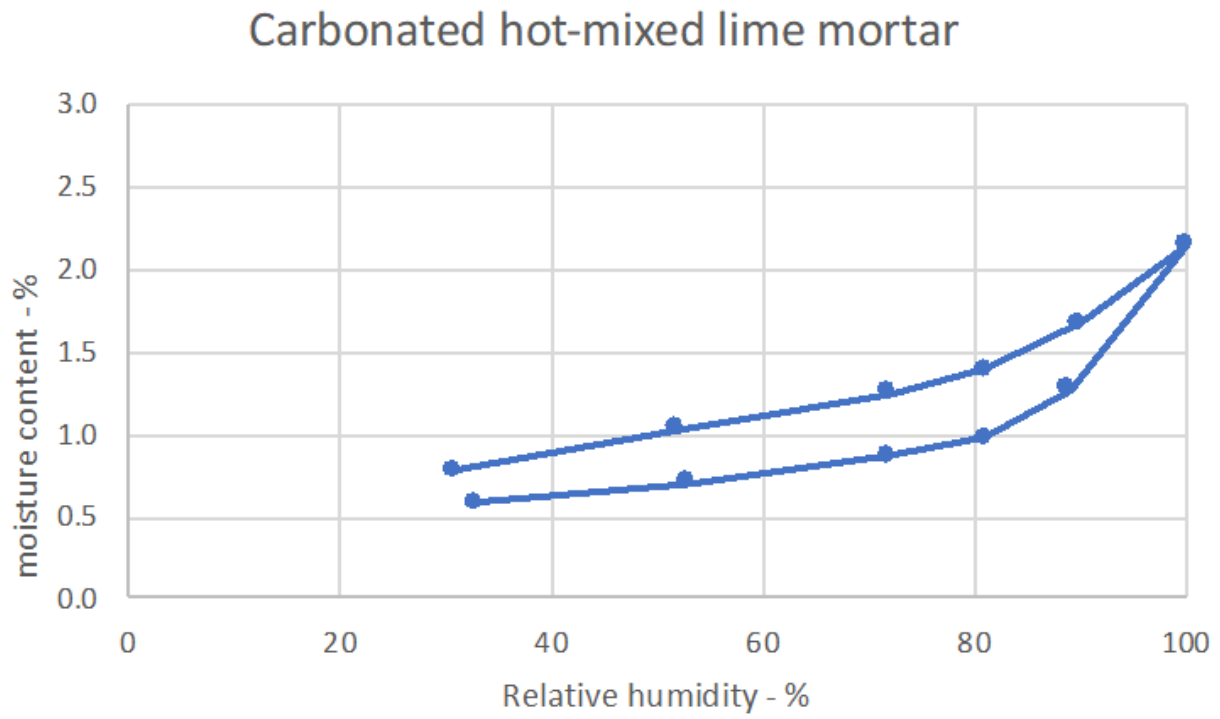


Figure 12 - Sorption-desorption curves for carbonated lime mortar.

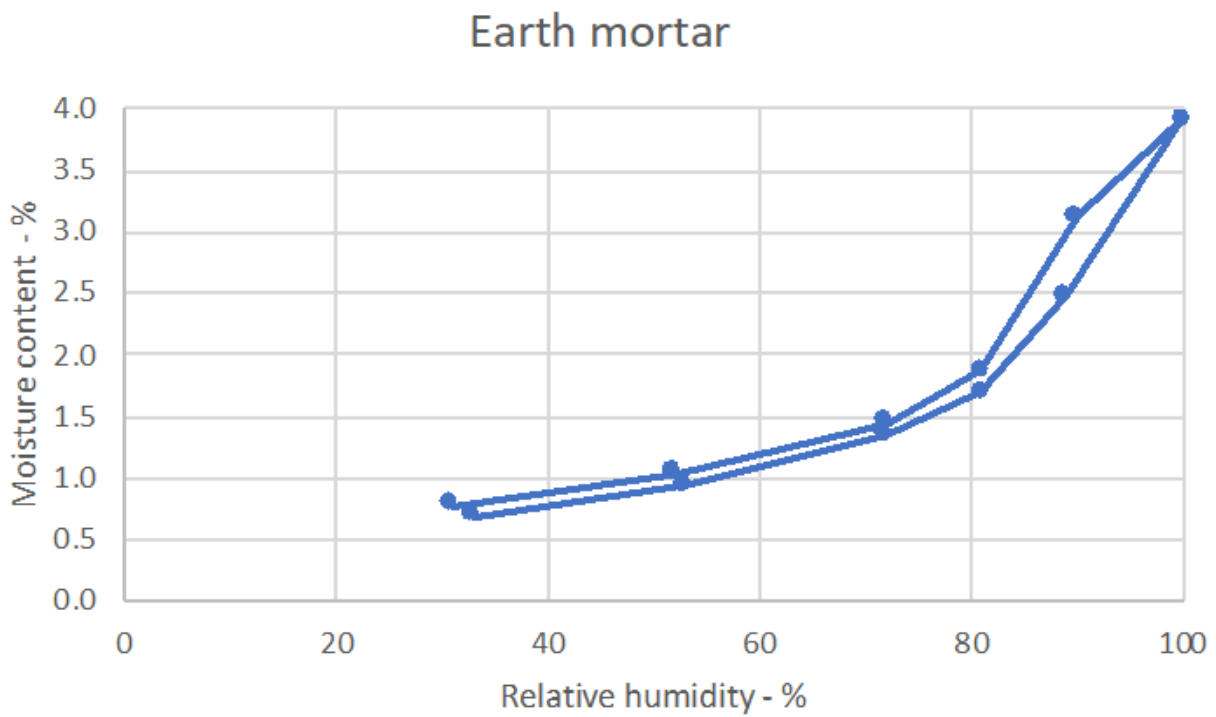


Figure 13 - Sorption-desorption curves for earth mortar.

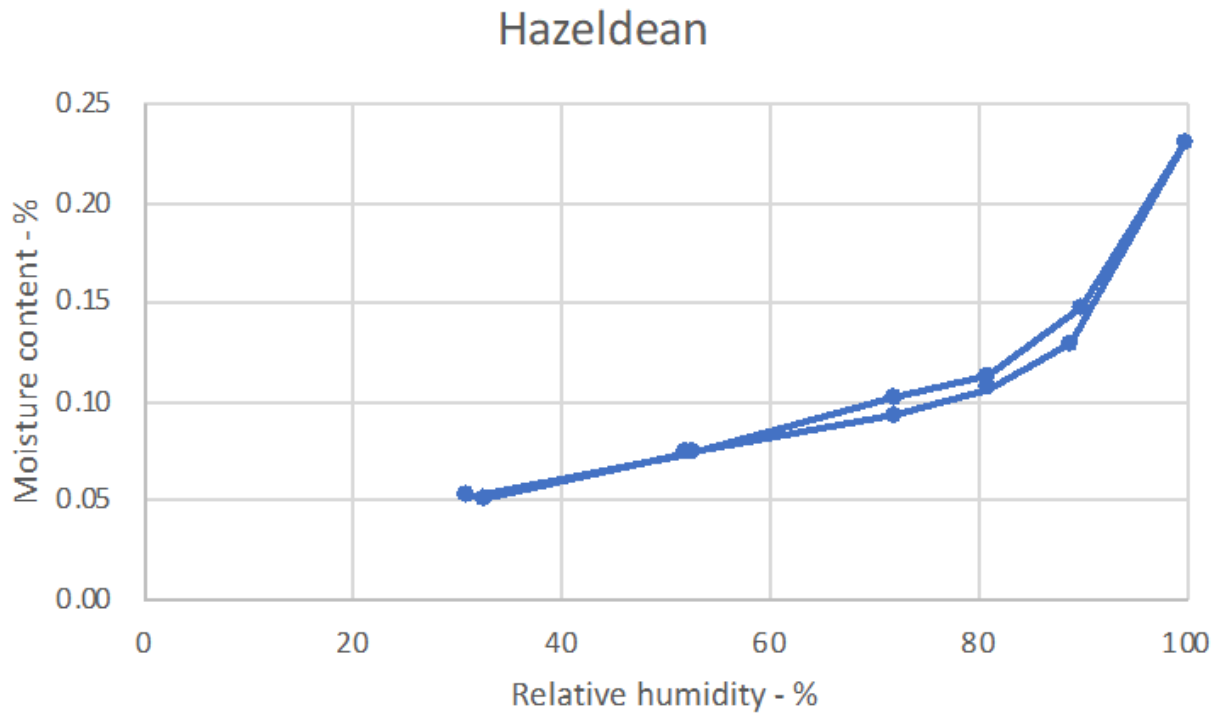


Figure 14 - Sorption-desorption curves for Hazeldean sandstone.

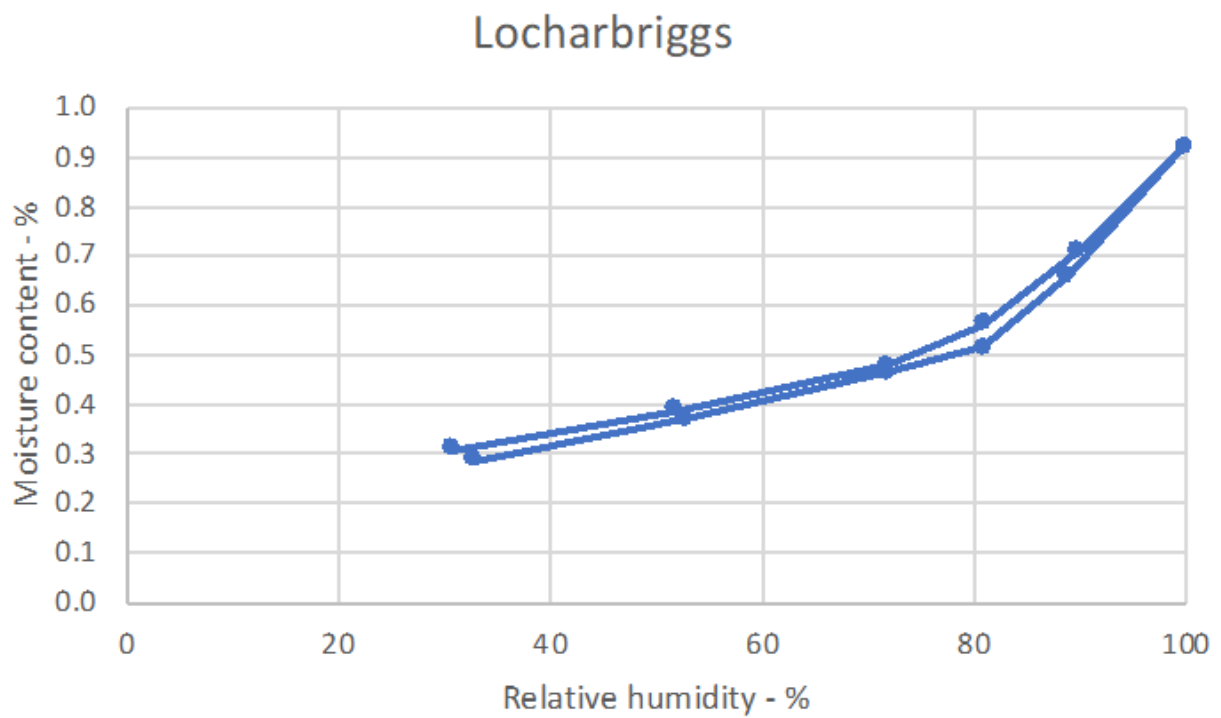


Figure 15 - Sorption-desorption curves for Locharbriggs sandstone.

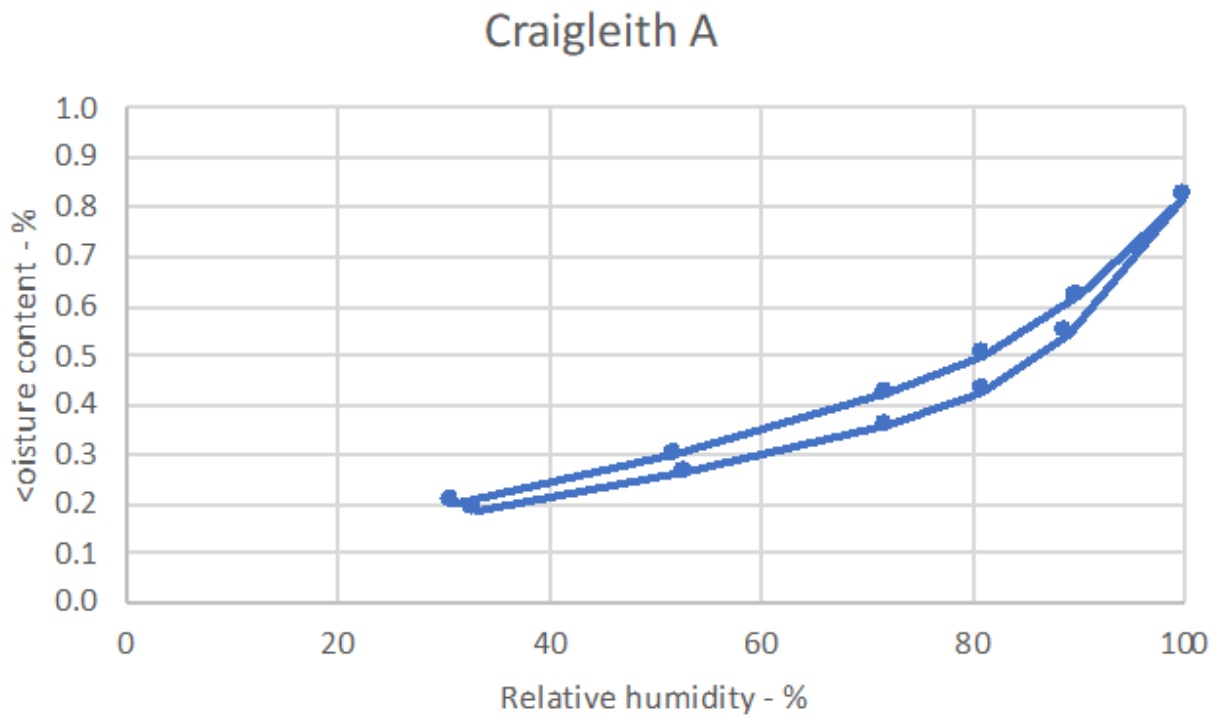


Figure 16 - Sorption-desorption curves for Craigleith A sandstone.

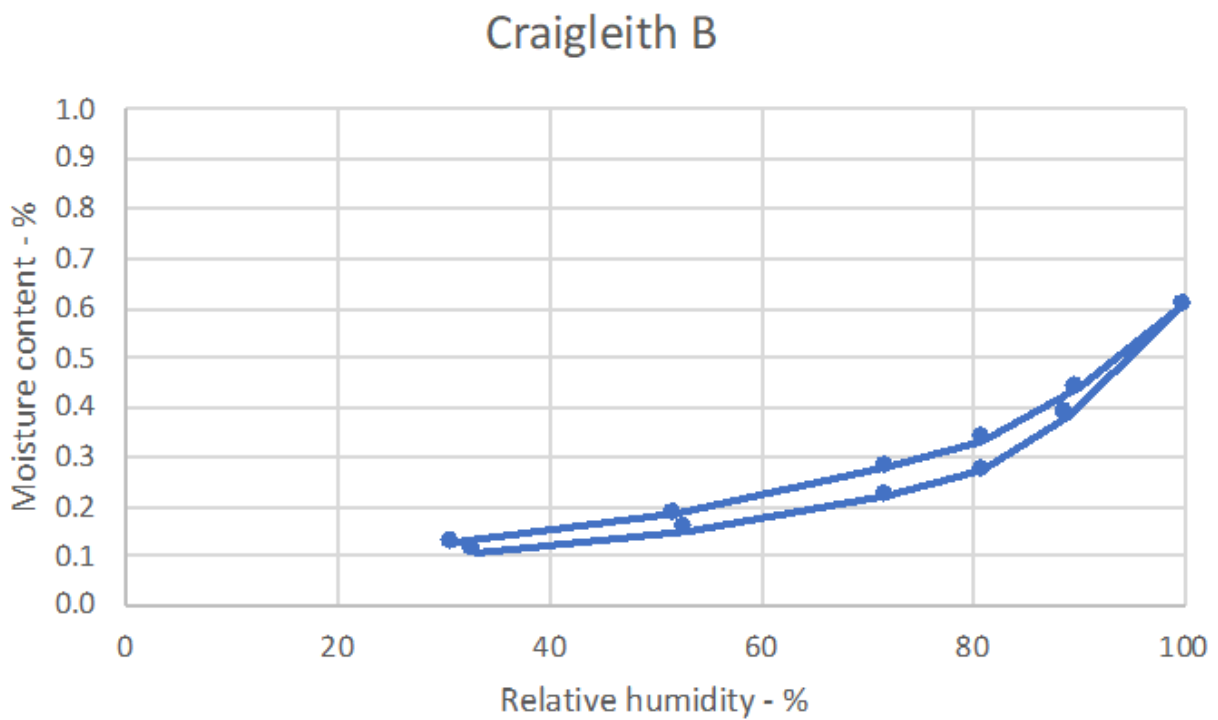


Figure 17 - Sorption-desorption curves for Craigleith B sandstone.

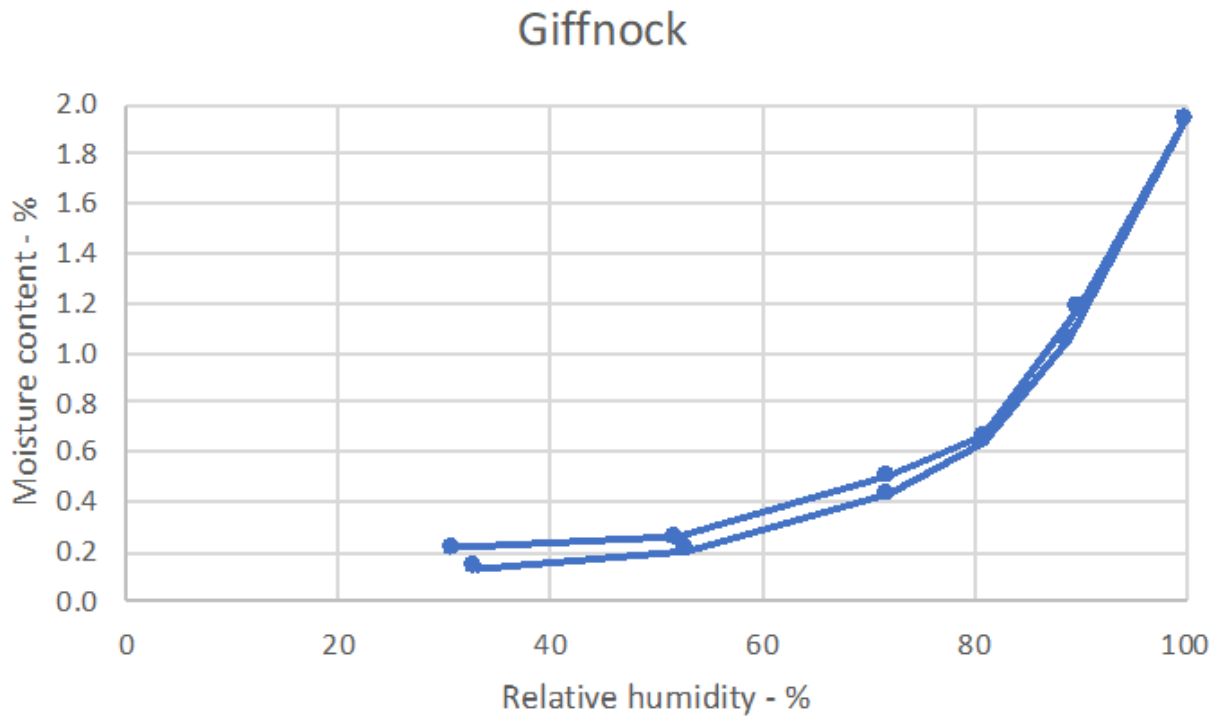


Figure 18 - Sorption-desorption curves for Giffnock sandstone.

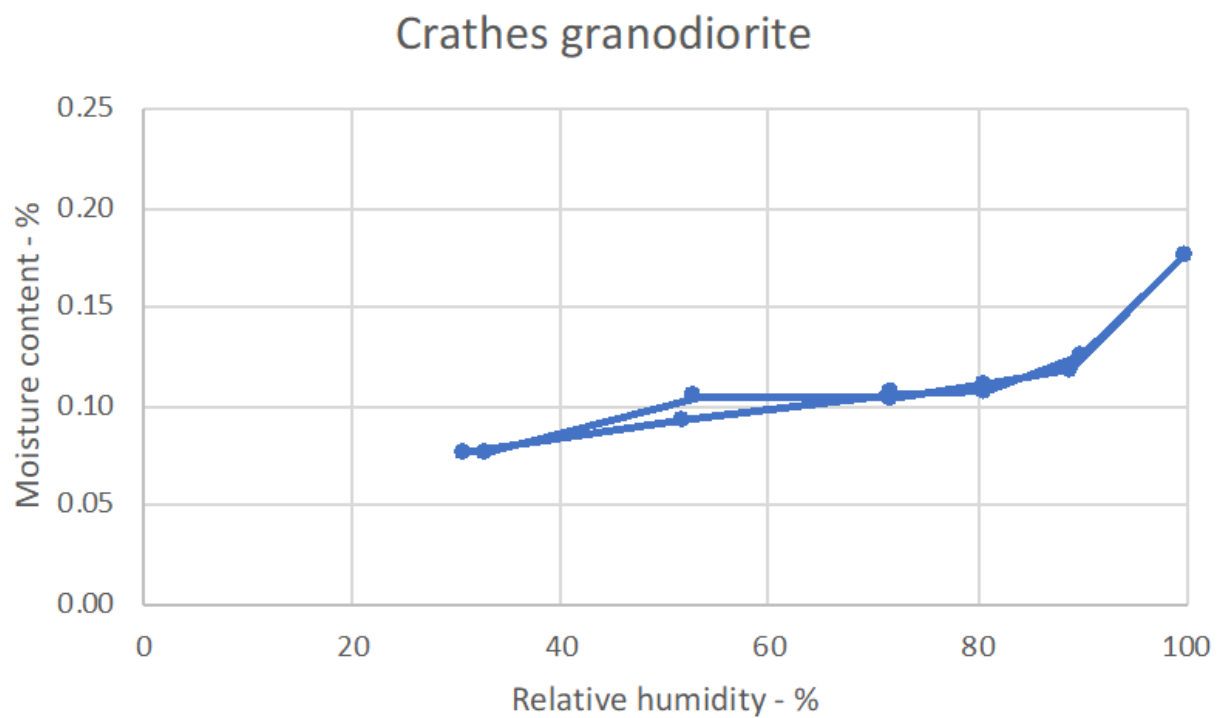


Figure 19 - Sorption-desorption curves for Crathes granodiorite.

For a consideration of the experimental error, the 3 replicates measured for RH for each material represent 220 df (11 points for each of 10 materials). The standard error is 0.067% moisture content, corresponding to a 90% confidence interval of about 0.11% moisture content.

The form of the sorption-desorption curves is the same for all materials, so to facilitate comparison, Table 5 summarises the moisture contents reached at a single point (90% RH), linearly interpolated on the upcurve.

Table 5 - Moisture contents of each material at 90% RH (upcurve, means of 3 specimens, all values $\pm 0.11\%$ moisture content).

Material	Moisture content at 90% RH	
	(% by mass)	(% by volume)
Uncarbonated lime mortar	1.48	2.62
Carbonated lime mortar	1.27	2.37
Earth mortar	2.48	4.97
Hazeldean sandstone	0.13	0.29
Locharbriggs sandstone	0.66	1.45
Craigleith A	0.54	1.33
Craigleith B	0.38	0.88
Giffnock sandstone	1.05	2.33
Scottish whinstone	-	-
Crathes granodiorite	0.12	0.31

The range of moisture contents varies 20-fold from highest to lowest. Using the confidence interval above, the materials may be grouped in the following order of hygroscopic sorption: earth mortar > uncarbonated and carbonated lime mortar > Giffnock sandstone > Locharbriggs sandstone > Craigleith A, Craigleith B > Hazeldean sandstone, Crathes granodiorite.

4.8. DENSITY

Table 6 summarises the density of each material in the oven-dry and saturated conditions, together with the moisture content (by mass and by volume) at saturation. The earth mortar specimens disintegrated on contact with water so the saturated density and the moisture content at saturation was not determined. For consideration of the experimental error associated with the values of density, there are 38 df and the standard error is 11.4, corresponding to a confidence interval of about $\pm 20 \text{ kg/m}^3$.

Table 6 - Density values in oven-dry and saturated conditions (means of 3 specimens).

Material	Density (dry)	Density (saturated)	Moisture content at saturation	
	(kg/m ³)	(kg/m ³)	% by mass	% by vol
Uncarbonated lime mortar	1762	1941	18.40	32.4
Carbonated lime mortar	1866	2008	15.53	29.0
Earth mortar	2002	-	-	-
Hazeldean sandstone	2273	2300	4.19	9.66
Locharbriggs sandstone	2192	2283	6.07	13.30
Craigleith A	2453	2489	1.82	4.52
Craigleith B	2300	2364	3.89	8.95
Giffnock sandstone	2208	2291	5.40	11.9
Scottish whinstone	2919	2925	0.21	0.61
Crathes granodiorite	2654	2658	0.21	0.56

From this analysis, the following features emerge: The dry densities are less widely spread than some of the other properties, covering a 1.65-fold range; The lime mortars have low density and the whinstone has high density, with the sandstones grouped in between. Using the confidence interval above, the materials may be grouped in the following order of dry density: Scottish whinstone> Crathes granodiorite> Craigleith A> Craigleith B, Hazeldean sandstones> Giffnock, Locharbriggs sandstones> earth mortar> carbonated lime mortar> uncarbonated lime mortar. As would be expected, the saturated moisture contents show the reverse order, with Scottish whinstone the least absorbent and uncarbonated lime mortar the most absorbent.

4.9. POROSITY

Figures 20-29 show the pore size distributions for each material in a form where the vertical axis is a quantitative measure of the volume of pores of the size given on the horizontal axis in logarithmic scale; it is important to note the different scales, however.

It should also be noted that the distribution curve for the earth mortar shows zero intrusion for small diameters, which suggests that the specimen collapsed under the high intruding mercury pressure.

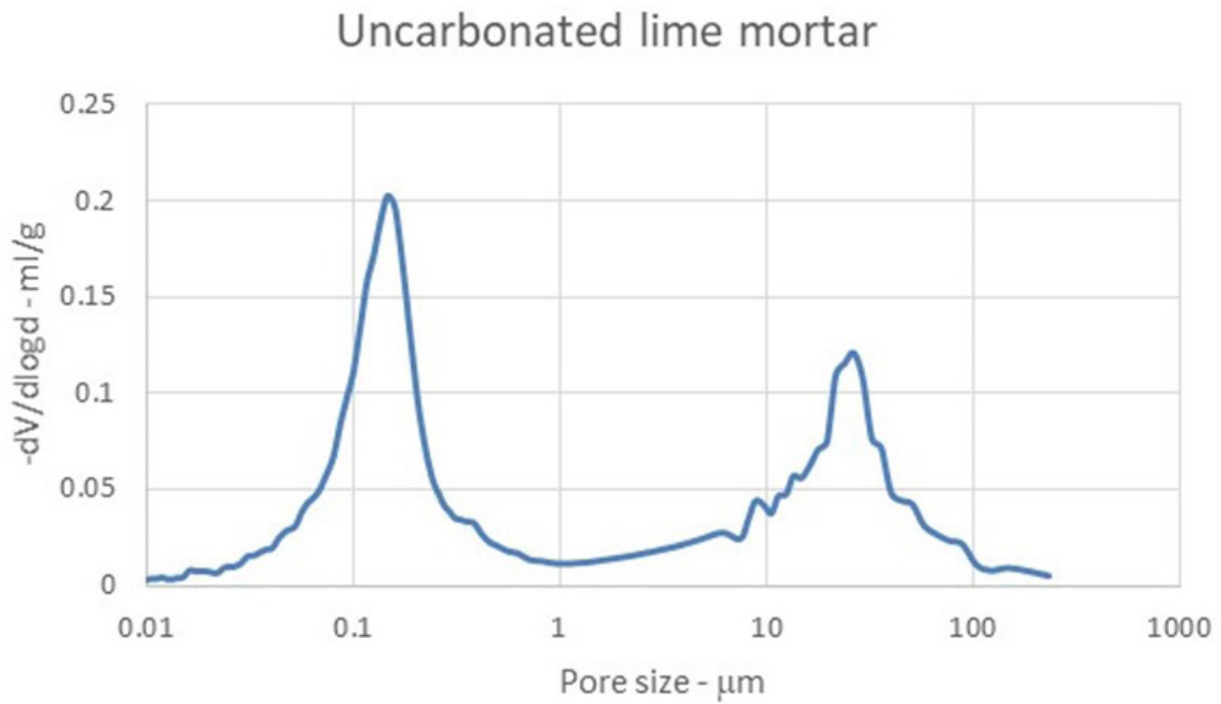


Figure 20 - Pore size distribution for uncarbonated lime mortar.

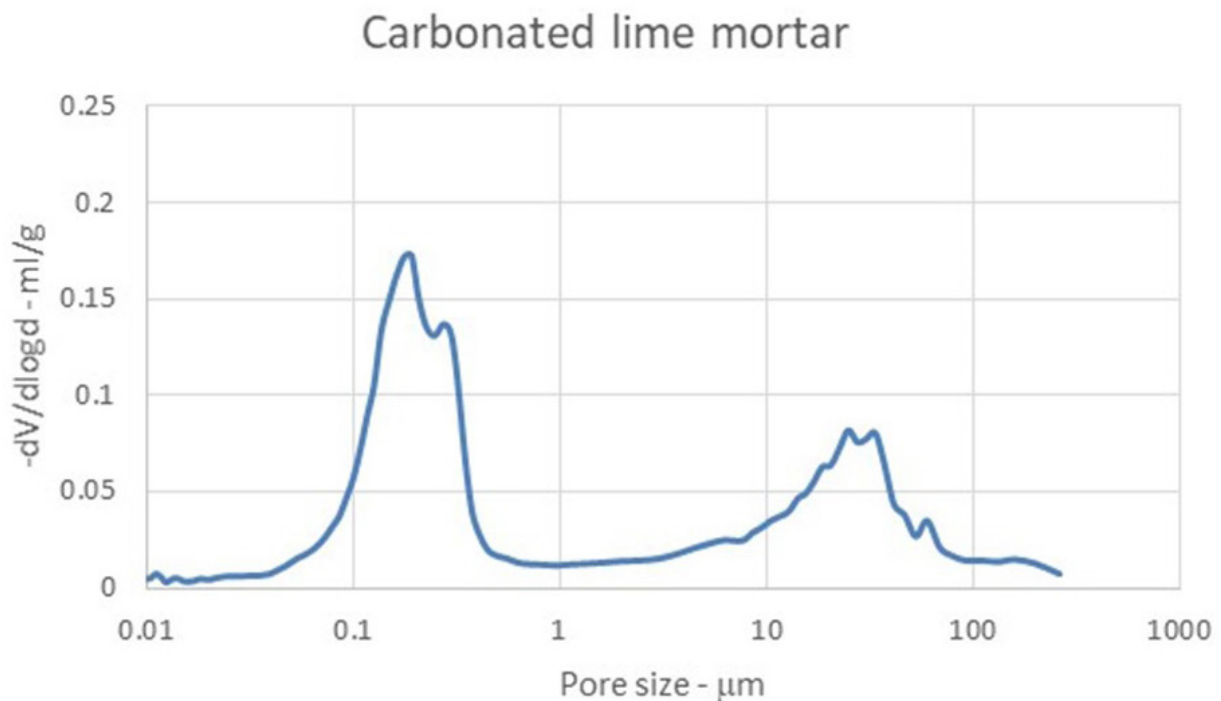


Figure 21 - Pore size distribution for carbonated lime mortar.

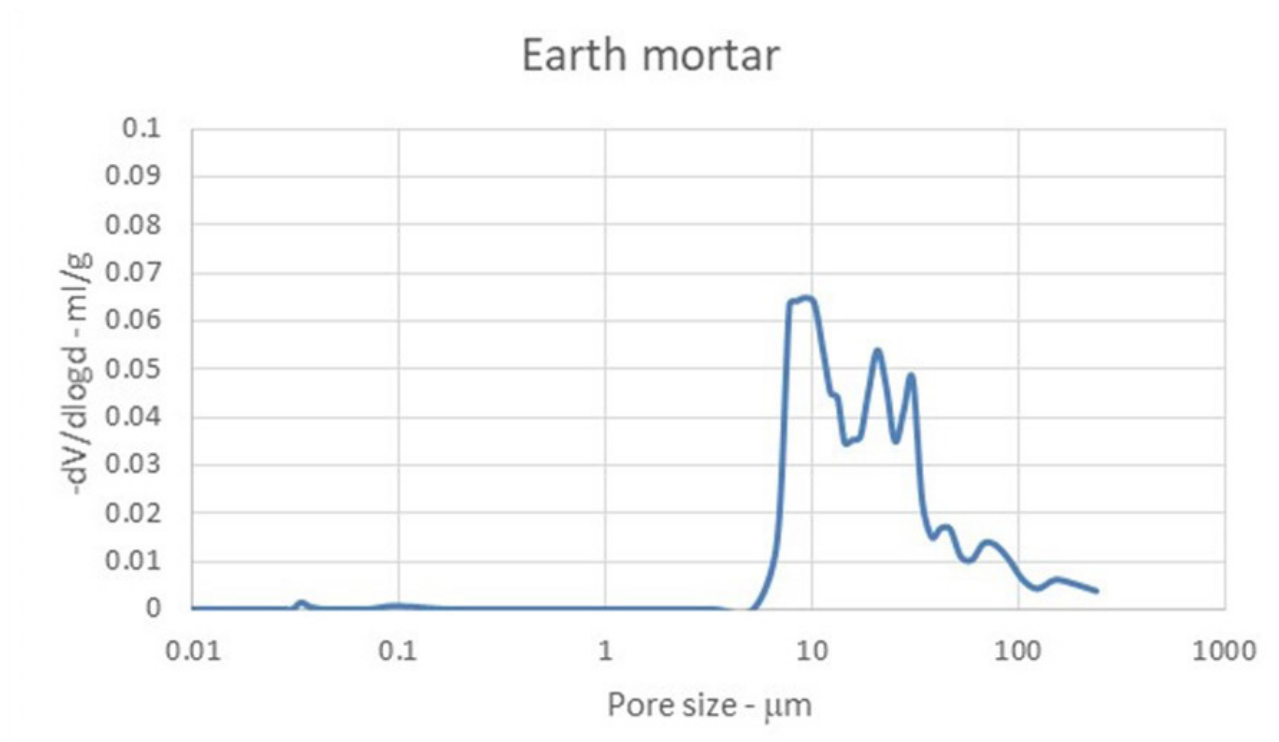


Figure 22 - Pore size distribution for earth mortar.

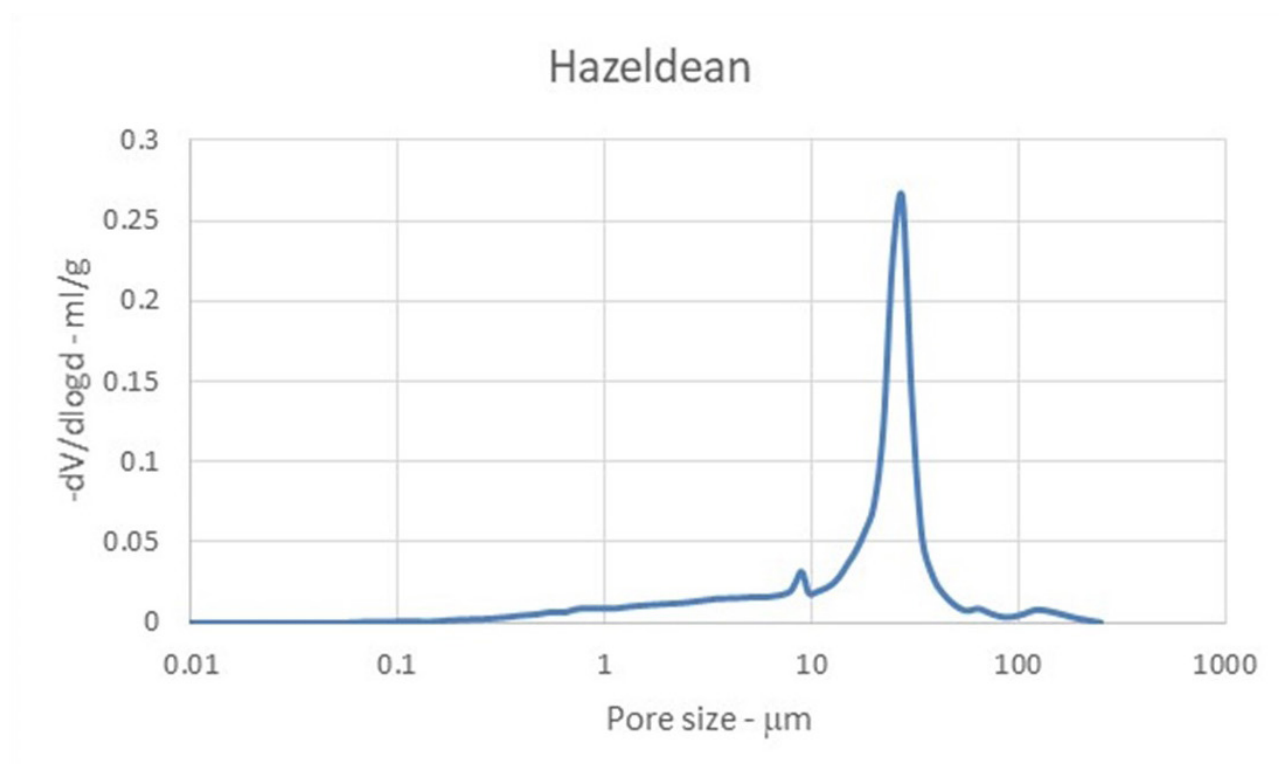


Figure 23 - Pore size distribution for Hazeldean sandstone.

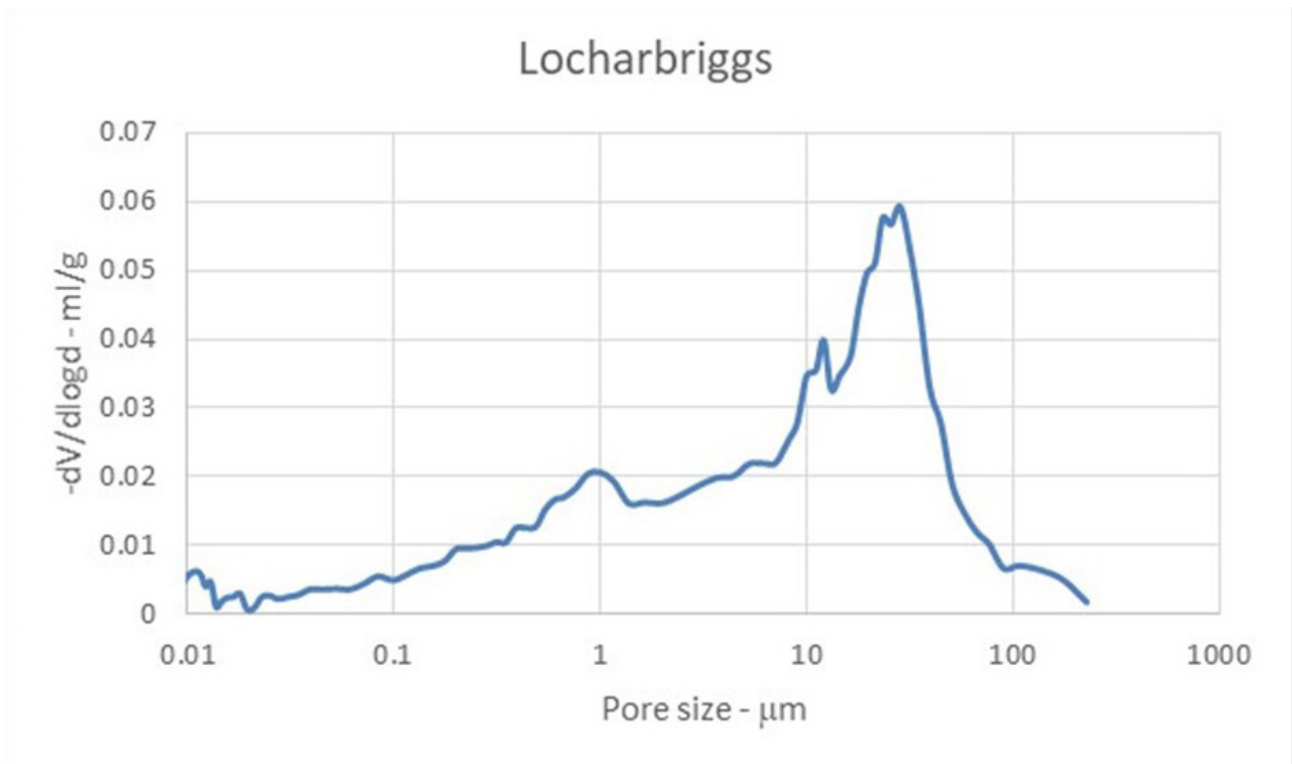


Figure 24 - Pore size distribution for Locharbriggs sandstone.

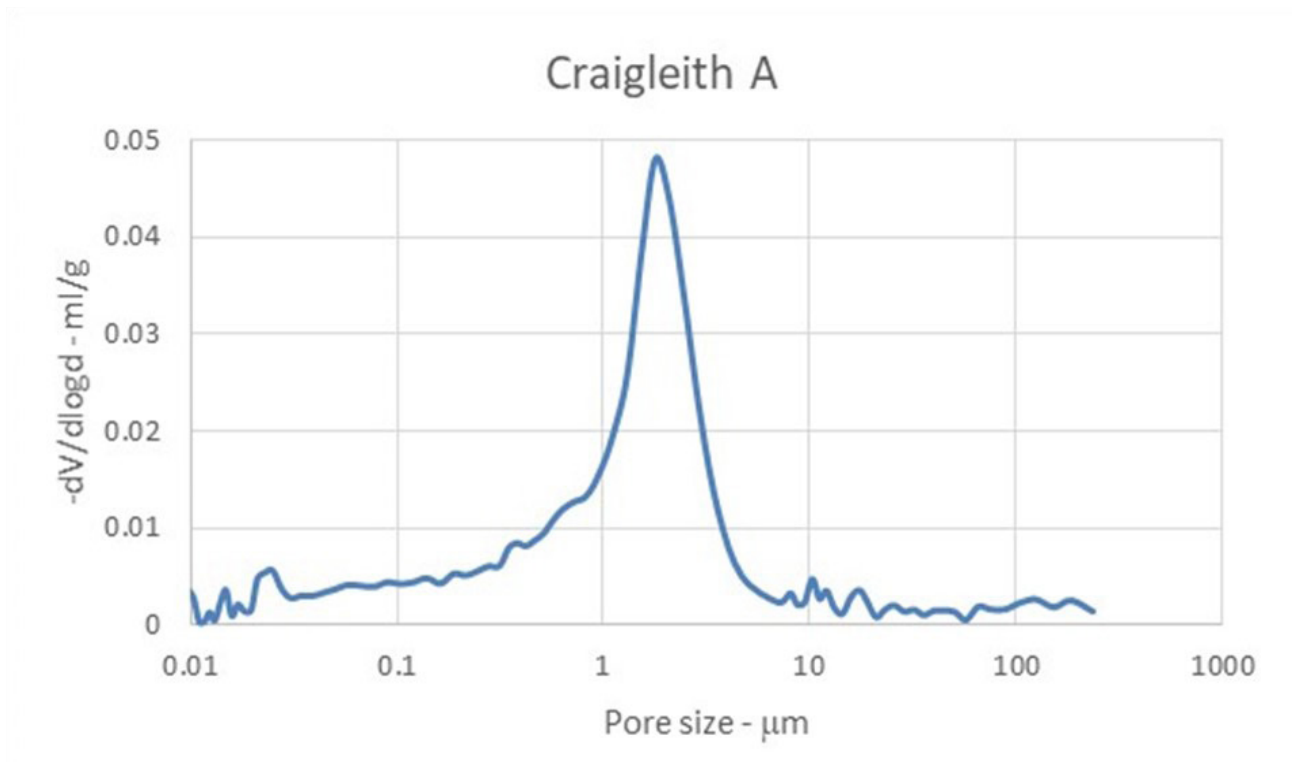


Figure 25 - Pore size distribution for Craigleith A sandstone.

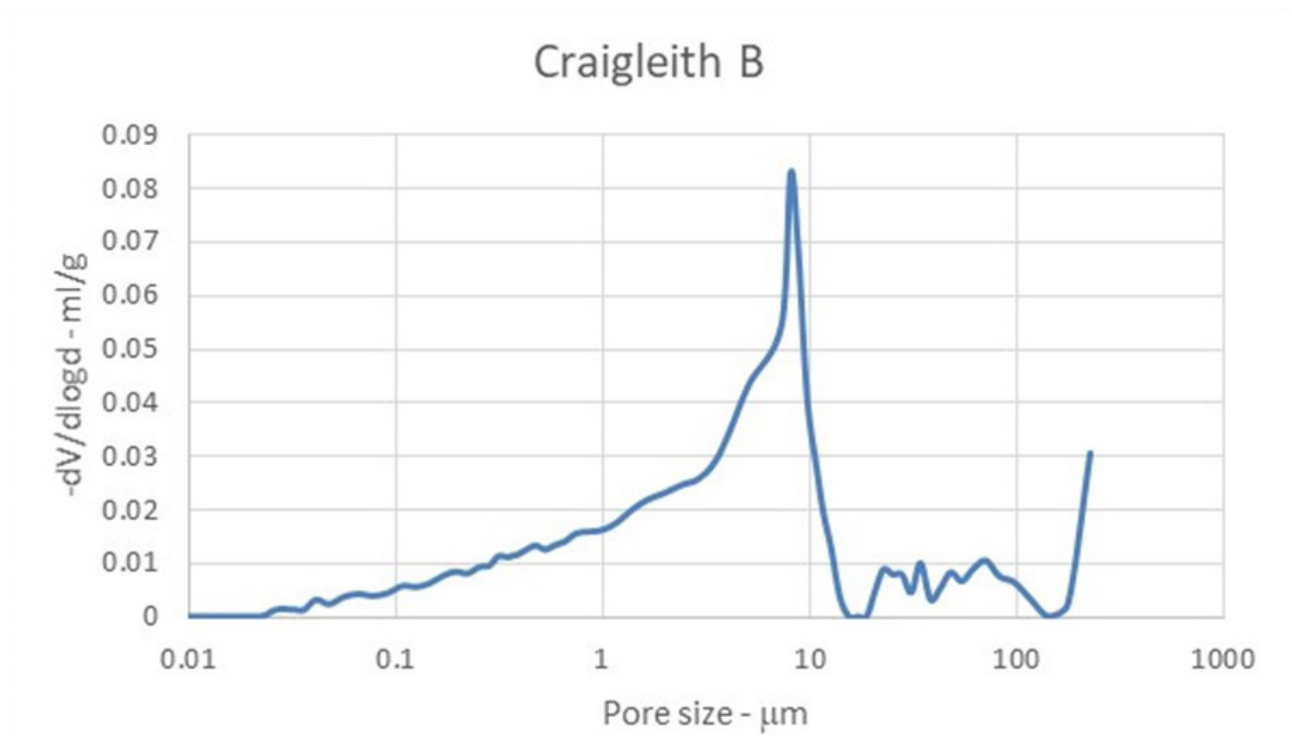


Figure 26 - Pore size distribution for Craigleith B sandstone.

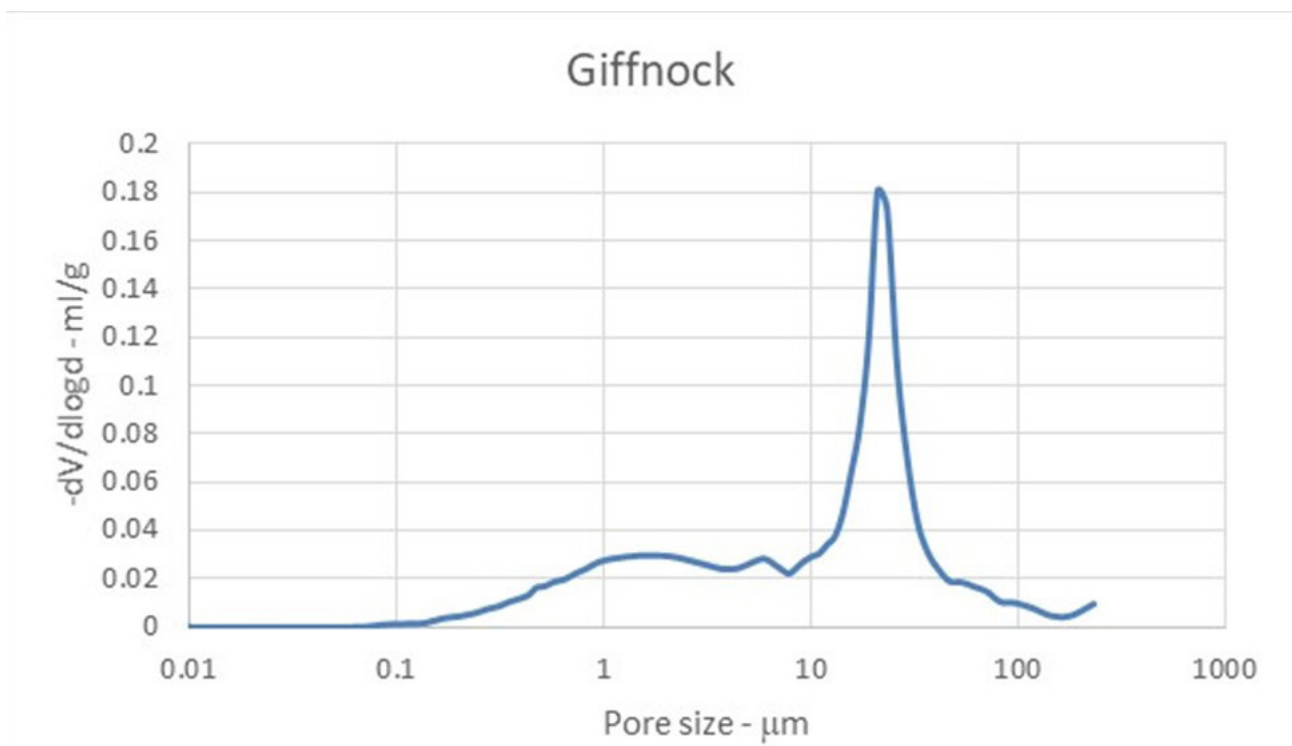


Figure 27 - Pore size distribution for Giffnock sandstone.

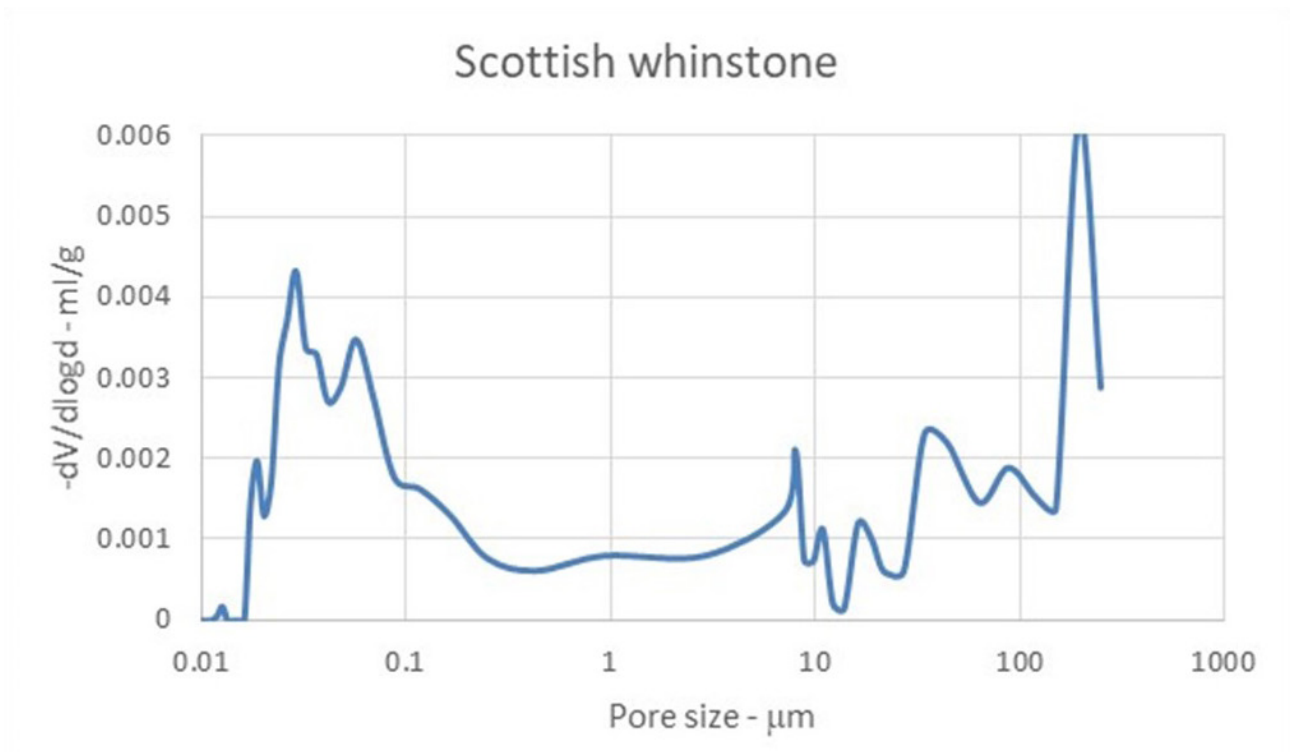


Figure 28 - Pore size distribution for Scottish whinstone.

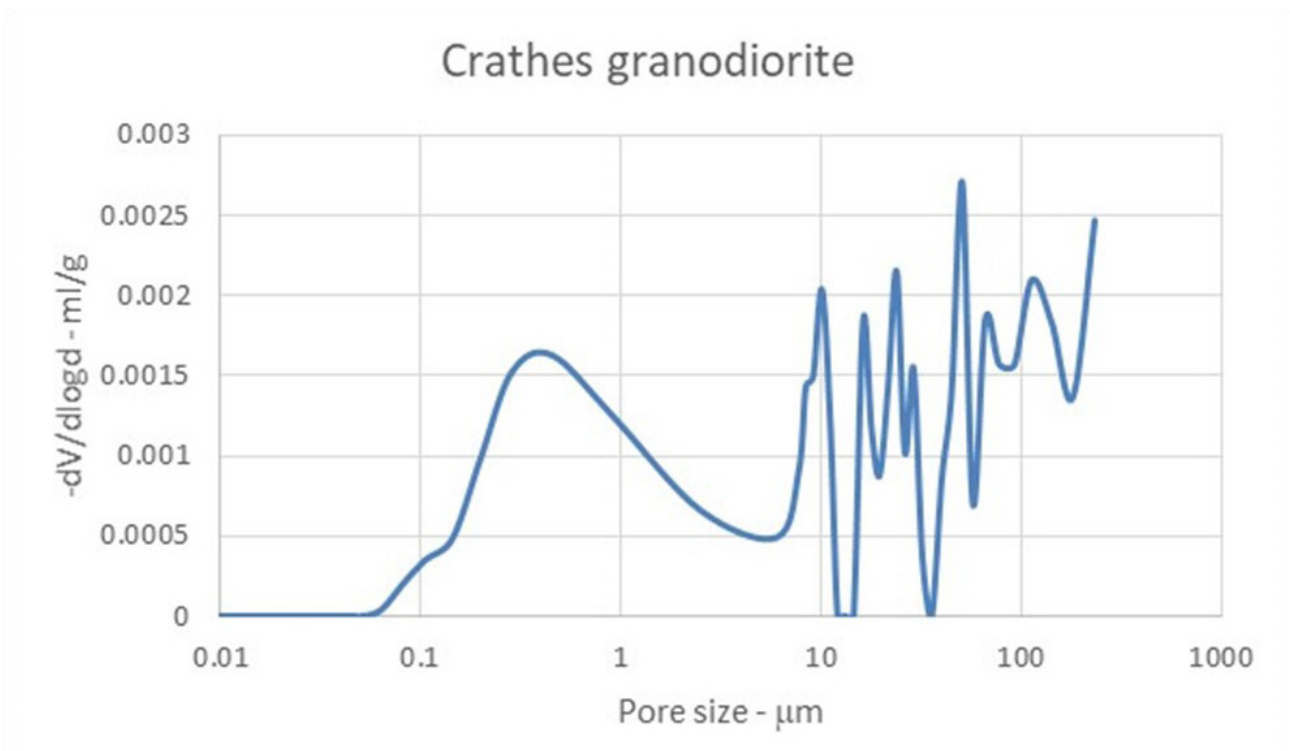


Figure 29 - Pore size distribution for Crathes granodiorite.

The lime mortars show a bimodal distribution, with the peak around 0.15-0.2 μm corresponding to the binder porosity, and that around 30 μm corresponding to the pores between sand particles. In contrast to what has been reported for Natural Hydraulic Lime mortars (Banfill, 2018), carbonation of the hot-mix lime mortar had little effect on the pore size distribution. Presumably, the earth mortar would have shown a similar bimodal distribution, but the collapse of the sample under pressure hides the lower peak. The sandstones all exhibit a well-defined main peak, with a shoulder at around 1 μm , which is clearly visible in the case of Locharbriggs and Giffnock, but less well-defined in Craigleith A and B, and absent in Hazeldean. In Locharbriggs, Hazeldean and Giffnock, the main peak lies around 28, 25 and 20 μm respectively, whilst in Craigleith A and B, the main peak reflects finer pores around 2 and 8 μm respectively. The whinstone and granodiorite have very low porosities with fine pores around 0.03 and 0.4 μm and with some poorly defined coarser pores between 10 and 150 μm .

Table 7 summarises the total porosities of each material. Additionally, the lime mortars can be divided into pore sizes below or above 10 μm , representing binder porosity and interparticle porosity, respectively. Both uncarbonated and carbonated lime mortar have 18.6% porosity below 10 μm with 12.65 and 11.4% respectively above 10 μm . If the earth mortar has a similar pore size distribution to that of the lime mortars, then its estimated total porosity is 20%.

Table 7 - Porosity (% by volume) of each material (single determination).

Material	Total porosity
Uncarbonated lime mortar	31.2
Carbonated lime mortar	30.0
Earth mortar	(20 estimated)
Hazeldean sandstone	17.3
Locharbriggs sandstone	15.7
Craigleith A	8.3
Craigleith B	13.2
Giffnock sandstone	20.8
Scottish whinstone	1.9
Crathes granodiorite	1.1

As expected, the lime mortars have a high total porosity and the granodiorite and whinstone have a low porosity, consistent with the high and low moisture contents at saturation recorded in Table 3. The sandstones occupy the middle range of porosity but with notable differences, which also reflect the various distributions in Figures 22-26. Craigleith A's low total porosity and vanishingly small coarse porosity are consistent with

its fine texture and good reputation as a durable sandstone. Craigleith B, Locharbriggs, Giffnock and Hazeldean sandstones have progressively higher proportions of coarse pores and the values, as well as the distributions, clearly show that it is wrong to assume that all sandstones are the same.

Comparing the total porosity determined by mercury intrusion (Table 7) with the saturated moisture content by volume in Table 6 confirms that the latter is lower than the former for every material. This is because mercury at high pressure is able to penetrate more pores than water at atmospheric pressure and is, therefore, a better estimate of total porosity. Even so, mercury intrusion is acknowledged to underestimate porosity because it cannot penetrate into sealed pores.

5 GENERAL DISCUSSION

The results described in the previous sections show that the differences between uncarbonated and carbonated hot-mix lime mortar are not significant. Of all the properties measured, only density differs by more than the confidence interval. Therefore, the following discussion does not differentiate between them and the term “hot-mix lime mortar” is taken to refer to either uncarbonated or carbonated.

5.1. VERACITY OF THE MEASURED DATA

To answer the question of whether the values reported here are realistic, this section compares them with those quoted in literature for similar materials. The task is hindered by the fact that few references report the whole range of material properties of interest and that, particularly for lime mortar, full information on the composition is often lacking. Accordingly, the comparison is restricted to four generic types of material – lime mortar, earth, sandstone and granite – and six properties – density (dry), thermal conductivity (dry), vapour diffusion resistance factor (dry cup tests), water absorption coefficient, hygroscopic sorption and porosity.

Tables 8-11 show the data for lime mortar, earth or earth mortar, sandstone and granite, respectively. The values for lime mortar are restricted to those that, in the cited reference, are either explicitly specified to be air-lime binders or for which no details are given. Natural hydraulic lime bound mortars are excluded. It can be noted that, for earth materials, Cagnon et al (2014) report on unfired earth bricks and WUFI (2020) gives values for clay mortar and soil of various kinds, but the latter give no details of the materials and it is not clear how some of them differ.

Table 8 - Comparison of data for lime mortars.

Parameter	This work	Other work	References
Density kg/m ³	1760-1880	1340-1810	Cerny et al, 2006; Cachova et al, 2016b; Lopez et al, 2017; Faria et al 2008; Vejmelkova et al, 2009; Padfield, 1998; IEA, 1991; WUFI, 2020
Thermal conductivity (dry) W/(m K)	0.2-0.22	0.35-1.4	Cachova et al, 2016b; Cerny et al, 2006; IEA, 1991; Vejmelkova et al, 2009; WUFI, 2020
Vapour diffusion resistance factor	23	6-37	Cachova et al, 2016b; Cerny et al, 2006; IEA, 1991; Lopez et al, 2017; Padfield, 1998; Vejmelkova et al, 2009; WUFI, 2020
Water absorption coefficient (kg/(m ² √s))	0.28-0.36	0.008-1.2	Cachova et al, 2016b; Cerny et al, 2006; Faria et al 2007; Loureiro et al, 2020; Vejmelkova et al, 2009; WUFI, 2020.

Hygroscopic sorption (% mc by volume at 90% RH)	2.4-2.6	0.17-1.6	Cachova et al, 2016b; IEA, 1991; Padfield, 1998; WUFI, 2020.
Total porosity %	30-31	26-49	Cachova et al, 2016b; Cerny et al, 2006; Faria et al 2007; IEA, 1991; Lopez et al, 2017; Loureiro et al, 2020; Vejmelkova et al, 2009; WUFI, 2020.

For lime mortar, every parameter except hygroscopic sorption falls within the range of other work, although the lowest density and highest porosity are for a single air lime mortar tested by Lopez et al. (2017). The next highest values of 1550 kg/m³ and 40% (Faria, 2008) are nearer to those found here. The affinity for moisture - manifested as hygroscopic sorption - of the hot-mix lime mortar in this work is significantly greater than that reported in other work. Pore diameters for four uncarbonated air lime mortars are given as 0.3-0.5µm and 20-80µm (Faria, 2008), similar to those shown in Figures 20-21.

Table 9 - Comparison of data for earth/earth mortars.

Parameter	This work	Other work	References
Density kg/m ³	2000	1570-2070	Cagnon et al, 2014; WUFI, 2020
Thermal conductivity (dry) W/(m K)	0.21	0.3-0.6	Cagnon et al, 2014; WUFI, 2020
Vapour diffusion resistance factor	29	7-19	Cagnon et al, 2014; WUFI, 2020
Water absorption coefficient (kg/(m ² √s))	-	0.18	WUFI, 2020
Hygroscopic sorption (% mc by volume at 90% RH)	5.0	0.2-15	Cagnon et al, 2014; WUFI, 2020.
Total porosity %	>8	-	

Compared to earth mortar, the earth bricks of Cagnon et al (2014) have similar density but higher thermal conductivity, lower vapour diffusion resistance factor and much higher hygroscopic sorption. In contrast, the clay mortar in WUFI (2020) has lower density, higher thermal conductivity, lower vapour diffusion resistance factor and higher hygroscopic sorption. Possibly the sand content of the earth mortar tested in this work makes comparison with these materials inappropriate. The water absorption coefficient of clay mortar in the WUFI database suggests it is similar to the hot-mix lime mortars tested in this work.

Table 10 - Comparison of data for sandstones.

Parameter	This work	Other work	References
Density kg/m ³	2200-2450	1925-2490	WUFI, 2020; Zhao & Plagge 2015
Thermal conductivity (dry) W/(m K)	1.1-1.7	1.0-3.5	IEA, 1991; Koci et al 2014; Mukhopadhyaya et al 2007; Vejmelkova et al 2013; WUFI, 2020
Vapour diffusion resistance factor	30-150	10-150	IEA, 1991; Koci et al 2014; Vejmelkova et al 2013; WUFI, 2020
Water absorption coefficient (kg/(m ² √s))	0.008-0.11	0.003-0.9	Krus, 1996; Mukhopadhyaya et al, 2007; Vejmelkova et al, 2013; WUFI, 2020; Zhao & Plagge 2015
Hygroscopic sorption (% mc by volume at 90% RH)	0.29-2.3	0.2-4.3	Abid et al, 2014; Makhlof et al, 2019; Vejmelkova et al, 2013; WUFI, 2020; Zhao & Plagge, 2015
Total porosity %	8-20	10-31	Abid et al, 2014; Haluk et al, 2019; Koci et al, 2014; Krus 1996; Makhlof et al, 2019; Vejmelkova et al, 2013; WUFI, 2020; Zhao & Plagge, 2015

For sandstone, every measured parameter falls within the range reported in other work, except for the total porosity of Craigleith sandstone, which is just below those reported elsewhere. Pore diameters of German sandstones are 0.1-0.3µm and 2-10µm (Zhao & Plagge, 2015), and of Czech sandstones 10-100µm (Vejmelkova et al, 2013), and those shown in Figures 23-27 are within this range.

Table 11 - Comparison of data for granite.

Parameter	This work	Other work	References
Density kg/m ³	2650	2450-3100	Ozcelik and Ozguven, 2014; IEA, 1991; WUFI, 2020
Thermal conductivity (dry) W/(m K)	2.1	1.6-4.1	IEA, 1991; WUFI, 2020
Vapour diffusion resistance factor	1350	54-60	IEA, 1991; WUFI, 2020
Water absorption coefficient (kg/(m ² √s))	0.011	0.0086	WUFI, 2020

Hygroscopic sorption (% mc by volume at 90% RH)	0.3	0.9	WUFI, 2020
Total porosity %	1.1	0.95-1.3	Ozcelik and Ozguven, 2014; WUFI, 2020

Only a single paper reporting data on granite has been located but density and thermal conductivity are within the range of other work and water absorption coefficient is similar. However, hygroscopic sorption and porosity are significantly less than given in WUFI (2020), which are consistent with granodiorite's much higher vapour diffusion resistance factor. Pore diameters are not given elsewhere.

The outcome of these comparisons suggests that the data reported in this work are broadly consistent with those reported elsewhere, particularly when the confidence intervals discussed above are taken into account, and there is, therefore, no reason to doubt the veracity of the values reported here.

5.2. APPLICATION OF THE INFORMATION TO HYGROTHERMAL SIMULATION

Whilst the laboratory work presented in this report has measured the relevant hygrothermal properties for WUFI simulation, it would be helpful to the practitioner to have the relevant data presented in the same format as the WUFI materials database. Accordingly, this section briefly discusses how WUFI uses hygrothermal property data for simulation, and data tables in the appropriate format are given in the Appendix. The author is grateful for helpful correspondence with Thomas Schmidt, Fraunhofer Institut für Bauphysik, Germany, in clarifying some matters.

For each material listed, the WUFI database quotes values of the following parameters in the units given: (i) bulk density (kg/m^3), (ii) porosity (m^3/m^3), (iii) specific heat capacity ($\text{J}/(\text{kg K})$), (iv) dry thermal conductivity ($\text{W}/(\text{m K})$), (v) vapour diffusion resistance factor (dimensionless) - dry cup, (vi) vapour diffusion resistance factor (dimensionless) - wet cup, (vii) moisture storage function, tabulated as water content (kg/m^3) at different relative humidities (dimensionless), (viii) liquid transport coefficient for suction, tabulated at different water contents, (ix) liquid transport coefficient for redistribution, tabulated at different water contents, (x) vapour diffusion resistance factor, tabulated at different RH (both dimensionless), (xi) thermal conductivity ($\text{W}/(\text{m K})$), tabulated at different water contents (kg/m^3), and (xii) thermal conductivity ($\text{W}/(\text{m K})$), tabulated at different temperatures ($^{\circ}\text{C}$). Whilst most of these parameters need no further comment other than to draw attention to the units used, some of them warrant further explanation in this section.

Specific heat capacity is not usually measured for materials in the WUFI database. This is not an important issue because hygrothermal simulations aim to determine water contents and not heat fluxes. Also, experience shows that the resulting water contents are not very sensitive to the choice of values for heat capacity. Therefore, WUFI considers that it is sufficient to use estimated values of $850 \text{ J}/(\text{kg K})$ for mineral materials and $1500 \text{ J}/(\text{kg K})$ for organic materials.

The table of the moisture storage function is built up from the values obtained in the hygroscopic sorption test (Figs. 11-19) at RHs up to 93%. It should be noted that Figures 11-19 show moisture content in % by mass, whereas WUFI uses kg/m^3 , which is numerically equal to ten times the % by volume, which in turn is obtained from % by mass multiplied by [bulk density divided by water density]. The table is completed by adding a value at 100% RH, taken from the free saturation moisture content by volume (Table 6). In a simulation, WUFI uses this information by linear interpolation between the points in the table.

The liquid transport coefficients for suction and redistribution refer to the movement of liquid water within the material. Suction refers to the situation where liquid water is in contact with the surface and the capillary forces draw the water into the pore system. The suction process is dominated by transport in the large pores which have low flow resistance and allow rapid transport. In contrast, redistribution refers to the situation where the surface has become dry and the empty pores try to draw the absorbed water out of full pores within the body of the material. This process is dominated by the smaller pores which have the higher capillary forces but also greater flow resistance. As a result, redistribution is a slow process and the liquid transport coefficient is smaller than that for suction. WUFI calculates the coefficient for suction D_{ws} at different water contents w from the water absorption coefficient A and the free water content at saturation w_f using the formula:

$$D_{ws} = 3.8 \left(\frac{A}{w_f} \right)^2 \times 1000 \left(\frac{w}{w_f} - 1 \right)$$

which assumes that the relationship is exponential. In the same way, WUFI assumes that the coefficient for redistribution is the same at low water content but a factor of ten lower at high water contents. This works satisfactorily in practice, but it is preferable to enter just the value of the water absorption coefficient and allow WUFI to calculate the coefficients for suction and redistribution, rather than to enter a table of data.

WUFI tabulates the vapour diffusion resistance factor from the two measurements (dry cup and wet cup) as a smoothed step function. The mean dimensionless RH in the dry cup test is 0.265 (i.e. mean of 0.03 and 0.5) and in the wet cup test 0.715 (0.5 and 0.93). This simplifies the computation for WUFI at the expense of slight inaccuracy.

Following all these considerations, the results presented in this report have been recast into tables of data in a “WUFI-friendly” format and these are tabulated for each material in the Appendix.

5.3. LIMITATIONS

As noted in the introduction, this exercise is a first attempt at providing data on Scottish masonry materials in a form suitable for hygrothermal simulation using WUFI or similar software. As a result, there are some limitations, which have been briefly discussed in the last chapters. First, the lime mortars used contemporary rather than historic binders, which means that the material properties reported are appropriate for new work. It would be necessary to perform careful non-destructive experimental work in a further

programme to obtain information on the properties of existing mortars in historic masonry. However, at least one of the references cited in Table 8 (Loureiro et al, 2020) gives data on historic lime mortars, which are in agreement with the contemporary binders tested here. This gives a measure of reassurance. Second, the measurements were made on single materials rather than layered or composite products. Whilst values can be combined when simulating a building (Little et al, 2015), further work on layered or composite products would be beneficial in confirming their work. Finally, it can be argued that the material sampling protocol gives no indication of the variability of each material. The replicate tests made on each sample of material give an indication of handling and testing variability but not, for example, of the variability between different parts of a quarry. This would require a more extensive sampling and testing programme than what has been practicable in this case, potentially involving the collection of many samples from one building or sampling a quarry's production over time.



6 CONCLUSION

The work described in this paper has provided new data to allow better hygrothermal simulation of traditional Scottish masonry and, importantly, mass masonry walls. As the retrofit imperative grows, better data for modelling is needed to assess hygrothermal risk and calculate the benefits of thermal improvements. Although the range of stone and mortars are limited, they are representative of the majority of building stones and mortar in Scotland: sandstones, whinstone, a granodiorite, a hot-mixed lime mortar and an earth mortar were all tested. The lab based work has allowed, through a series of experiments, to determine the values of water vapour permeability and vapour diffusion resistance factor (by both dry cup and wet cup methods), thermal conductivity, water sorptivity/absorption coefficient, hygroscopic sorption, density and porosity for these materials. As a result, hygrothermal simulation software can be used with more confidence. Although there were some limitations to this exercise and further testing could provide more accurate results, it is a necessary start to building up full data to allow more accurate hygrothermal modelling of Scottish construction materials.



7 CONTACTS

**Historic Environment Scotland
Conservation
(technical advice)**

Longmore House, Salisbury Place, Edinburgh, EH9 1SH T: 0131 668 8668

E: technicalresearch@hes.scot

W: <https://www.historicenvironment.scot/>

**Historic Environment Scotland
Heritage Management
(planning/listed building matters)**

Longmore House, Salisbury Place, Edinburgh, EH9 1SH T: 0131 668 8716

E: hmenquiries@hes.scot

W: <https://www.historicenvironment.scot/>

**Historic Environment Scotland
(grants)**

Longmore House, Salisbury Place, Edinburgh, EH9 1SH T: 0131 668 8801

E: grants@hes.scot

W: <https://www.historicenvironment.scot/>

8 BIBLIOGRAPHY

- Abid, M., Hammerschmidt, U. and Kohler, J. (2014) 'Temperature and moisture dependent thermophysical properties of Sander sandstone', *International Journal of Thermal Sciences*, 86, pp. 88-94.
- ASTM (2014) *D5334-14: Standard test method for determination of thermal conductivity of soil and soft rock by thermal needle probe procedure*, West Conshohocken, USA: ASTM International.
- Banfill, P.F.G. (2018) 'Hygrothermal properties of NHL mortars', in Broström, T. and Nilsen, L. (eds.) *Proceedings of the 3rd International Conference on Energy Efficiency in Historic Buildings (EEHB2018)*, Visby, Sweden, 2018, pp. 71-79.
- BSI (2001) *BS EN ISO 12572:2001: Hygrothermal performance of building materials and products – Determination of water vapour transmission properties*. London: British Standards Institution.
- BSI (2002) *BS EN ISO 15148:2002: Hygrothermal performance of building materials and products – Determination of water absorption coefficient by partial immersion*. London: British Standards Institution.
- BSI (2007) *BS EN 10456:2007: Building materials and products. Hygrothermal properties. Tabulated design values and procedures for determining declared and design thermal values*. London: British Standards Institution.
- BSI (2013) *BS EN ISO 12571:2013: Hygrothermal performance of building materials and products – Determination of hygroscopic sorption properties*. London: British Standards Institution.
- Cachova, M., Koatkova, J., Konakova, D., Vejmelkova, E., Bartonkova, E. and Cerny, R. (2016a) 'Hygric properties of lime-cement plasters with the addition of pozzolana', *Procedia Engineering*, 151, pp. 127-132.
- Cachova, M., Vejmelkova, E., Konakova, D., Zumar, J., Keppert, M., Reiterman, P. and Cerny, R. (2016b) 'Application of ceramic powder as supplementary cementitious material in lime plasters', *Materials Science (Medziagotyra)*, 22, pp. 440-444.
- Cagnon, H., Aubert, J.E., Coutand, M. and Magniont, C. (2014) 'Hygrothermal properties of earth bricks', *Energy and Buildings*, 80, pp. 208-217.
- Cerny, R., Kunca, A., Tydlitát, V., Drchalova, J. and Rovnanikova, P. (2006) 'Effect of pozzolanic admixtures on mechanical, thermal and hygric properties of lime plasters', *Construction and Building Materials*, 20, pp. 849-857.
- Chatfield, C. (1970) *Statistics for technology*. London: Chapman and Hall.
- Davies, O.L. (1957) *Design and analysis of industrial experiments*. London: Oliver and Boyd.
- Faria, P., Henriques, F. and Rato, V. (2008) 'Comparative evaluation of lime mortars for architectural conservation', *Journal of Cultural Heritage*, 9, pp. 338-346.
- Fusade, L., Viles, H., Wood, C. and Burns, C. (2019) 'The effect of wood ash on the properties and durability of lime mortar for repointing damp historic buildings', *Construction and Building Materials*, 212, pp. 500-513.
- Haluk Selim, H., Karakas, A. and Coruk, O. (2019) 'Investigation of engineering properties for usability of Lefke stone (Osmaneli/Bilecik) as building stone', *Bulletin of Engineering Geology and the Environment*, 78, pp. 6047-6059.
- IEA (1991) *Catalogue of material properties: Annex 14, volume 3, Condensation and Energy*. Paris: International Energy Agency.
- Jenkins, M. and Curtis, R. (2014) *Inform Guide: Improving energy efficiency in traditional buildings*. Edinburgh: Historic Environment Scotland. Available at: <https://www.historicenvironment.scot/archives-and-research/publications/publication/?publicationid=246f4ae-1483-452a-8fb3-a59500bd05d5> [Accessed 17 February 2021].

-
- Kaye, G.W.C. and Laby, T.H. (1966) *Tables of physical and chemical constants*. London: Longman.
- Koci, V., Madera, J., Fort, J., Zumar, J., Pavlikova, M., Pavlik, Z. and Cerny, R. (2014) 'Service life assessment of historical building envelopes constructed using different types of sandstone: a computational analysis based on experimental input data', *Science World Journal*, 1, pp. 1-12.
- Krus, M. (1996) *Moisture transport and storage coefficients of porous mineral building materials*. Stuttgart: Fraunhofer IRB Verlag.
- Künzel, H.M. (1995) *Simultaneous heat and moisture transport in building components: One- and two-dimensional calculation using simple parameters*. Holzkirchen: Fraunhofer Institute of Building Physics.
- Little, J, Ferraro, C. and Arregi, B. (2015) *Technical Paper 15: Assessing risks in insulation retrofits using hygrothermal software tools*. Edinburgh: Historic Environment Scotland.
- Lopez, O., Torres, I., Guimares, A.S., Delgado, J.M.P.Q. and de Freitas, V.P. (2017) 'Inter-laboratory variability results of porous building materials hygrothermal properties', *Construction and Building Materials*, 156, pp. 412-423.
- Loureiro, A.M.S., da Paz, S.P.A., Veiga, M.R. and Angelica, R.S. (2020) 'Investigation of historical mortars from Belem do Para, Northern Brazil', *Construction and Building Materials*, 233, p. 117284.
- Makhlouf, N.N., Maskell, D., Marsh, A., Natarajan, S., Dabaieh, M. and Afify, M.M. (2019). 'Hygrothermal performance of vernacular stone in a desert climate', *Construction and Building Materials*, 216, pp. 687-696.
- McCaig, I., Pender, R. and Pickles, D. (2018) *Energy efficiency and historic buildings – how to improve energy efficiency*. London: Historic England. Available at: <https://historicengland.org.uk/energyefficiency> [Accessed 17 February 2021].
- MHCLG (2019) *Resistance to moisture in buildings: Using numerical simulation to assess moisture risk in retrofit constructions*. London: Ministry of Housing, Communities and Local Government. Available at: <https://www.gov.uk/government/publications/resistance-to-moisture-in-buildings> [Accessed 11 February 2021].
- Mukhopadhyaya, P., Kumaran, M.K., Lackey, J., Normandin, N., van Reenen, D. and Tariku, F. (2007) 'Hygrothermal properties of exterior claddings, sheathing boards, membranes and insulation materials for building envelope design', in *Proceedings of Thermal Performance of the Exterior Envelopes of Whole Buildings X, Clearwater, FL*, pp. 1-16.
- Ozcelik, Y. and Ozguven, A. (2014) 'Water absorption and drying features of different natural building stones', *Construction and Building Materials*, 63, pp. 257-270.
- Padfield, T. (1998) *The role of absorbent building materials in moderating changes of relative humidity*. PhD Thesis, Technical University of Denmark.
- Prince's Regeneration Trust (2015) *The green guide for historic buildings: How to improve the environmental sustainability of listed and historic buildings*. London: The Stationery Office,
- SLCT (2019) *AP3449: Stone analysis and matching report. Old College Edinburgh*. Charlestown: Scottish Lime Centre Trust.
- Vejmelkova, E., Pernicova, R., Sovjak, R. and Cerny, R. (2009) 'Properties of innovative renders on a lime basis for the renovation of historical buildings', *WIT Transactions on the Built Environment*, 109, pp. 221-229.
- Vejmelkova, E., Keppert, M., Reiterman, P. and Cerny, R. (2013) 'Mechanical, hygric and thermal properties of building stones', *WIT Transactions on the Built Environment*, 131, 357-367.
- WUFI (2020) *Wärme und Feuchte Instanzionär*. www.wufi.de [Accessed 18 December 2020].
- Zhao, J. and Plagge, R. (2015) 'Characterization of hygrothermal properties of sandstones – Impact of anisotropy on their thermal and moisture behaviors', *Energy and Buildings*, 107, pp. 479-494.

9 HES TECHNICAL CONSERVATION PUBLICATION SERIES

The following publications are all free to download and are available from the publications page on our website: <https://www.historicenvironment.scot/archives-and-research/publications/>

Technical Papers

Our Technical Papers series disseminates the results of research carried out or commissioned by Historic Environment Scotland, mostly related to improving energy efficiency in traditional buildings. This series covers topics such as thermal performance of traditional windows, U-values and traditional buildings, keeping warm in a cool house and slim-profile double-glazing.

Refurbishment Case Studies

This series details practical applications concerning the repair and upgrade of traditional structures to improve thermal performance. The Refurbishment Case Studies are projects sponsored by Historic Environment Scotland and the results are part of the evidence base that informs our technical guidance. This series covers measures such as upgrades to windows, walls and roof spaces in a range of traditional building types such as tenements, cottages and public buildings.

INFORM Guides

Our INFORM Guides provide short introductions to a range of topics relating to traditional skills and materials, building defects and the conservation and repair of traditional buildings. This series covers topics such as: ventilation in traditional houses, maintaining sash and case windows, domestic chimneys and flues, damp causes and solutions improving energy efficiency in traditional buildings and biological growth on masonry.

Short Guides

Our Short Guides are more in-depth guides, aimed at practitioners and professionals, but may also be of interest to contractors, home owners and students. The series provides advice on a range of topics relating to traditional buildings and skills.

APPENDIX: TABLES OF VALUES FOR USE IN WUFI

Table A1 - Hot-mixed lime mortar (both uncarbonated and carbonated).

Material	Hot-mixed lime mortar					Any other information		Data from Heriot-Watt University						
	Bulk density kg/m ³	Porosity m ³ /m ³	Heat capacity J/kgK	Thermal conductivity dry W/mK	Vapour diffusion resistance factor - dry cup	Vapour diffusion resistance factor - wet cup	Moisture storage function		Water absorption coefficient kg/m ² /s	Vapour diffusion resistance factor - relative humidity dependent		Thermal conductivity - moisture dependent		Thermal conductivity - temperature dependent
						Relative humidity dimensionless	Water content kg/m ³		Relative humidity dimensionless	mu-value dimensionless	Water content kg/m ³	Thermal conductivity W/mK	Temp °C	Thermal conductivity W/mK
1810	0.3	850*	0.2	23	14	0	0	0.32	0	23	0	0.2	20	0.2
						0.33	12.6		0.265	23	307	0.7		
						0.53	14.6		0.715	14				
						0.72	15.6		1	14				
						0.81	18.1							
						0.89	25							
						1	307							

*Assumed value, not measured

Table A2 - Earth mortar.

Material	Earth mortar					Any other information		Data from Heriot-Watt University						
	Bulk density kg/m ³	Porosity m ³ /m ³	Heat capacity J/kgK	Thermal conductivity dry W/mK	Vapour diffusion resistance factor - dry cup	Vapour diffusion resistance factor - wet cup	Moisture storage function		Water absorption coefficient kg/m ² /s	Vapour diffusion resistance factor - relative humidity dependent		Thermal conductivity - moisture dependent		Thermal conductivity - temperature dependent
						Relative humidity dimensionless	Water content kg/m ³		Relative humidity dimensionless	mu-value dimensionless	Water content kg/m ³	Thermal conductivity W/mK	Temp °C	Thermal conductivity W/mK
2000	0.2	850*	0.2	29	12	0	0		0	29	0	0.2	20	1.5
						0.33	13.8		0.265	29	0	0.2		
						0.53	18.9		0.715	12				
						0.72	27.1		1	12				
						0.81	33.9							
						0.89	49.7							
						1	200*							

*Assumed value, not measured

Table A3 - Hazeldean sandstone.

Material	Hazeldean sandstone					Any other information		Data from Heriot-Watt University						
	Bulk density kg/m ³	Porosity m ³ /m ³	Heat capacity J/kgK	Thermal conductivity dry W/mK	Vapour diffusion resistance factor - dry cup	Vapour diffusion resistance factor - wet cup	Moisture storage function		Water absorption coefficient kg/m ² /s	Vapour diffusion resistance factor - relative humidity dependent		Thermal conductivity - moisture dependent		Thermal conductivity - temperature dependent
						Relative humidity dimensionless	Water content kg/m ³		Relative humidity dimensionless	mu-value dimensionless	Water content kg/m ³	Thermal conductivity W/mK	Temp °C	Thermal conductivity W/mK
2270	0.17	850*	1.7	37	22	0	0	0.11	0	37	0	1.7	20	1.7
						0.33	1.2		0.265	37	97	4		
						0.53	1.7		0.715	22				
						0.72	2.1		1	22				
						0.81	2.4							
						0.89	2.9							
						1	96.6							

*Assumed value, not measured

Table A4 - Locharbriggs sandstone.

Material	Locharbriggs sandstone					Any other information		Data from Heriot-Watt University						
	Bulk density kg/m ³	Porosity m ³ /m ³	Heat capacity J/kgK	Thermal conductivity dry W/mK	Vapour diffusion resistance factor - dry cup	Vapour diffusion resistance factor - wet cup	Moisture storage function		Water absorption coefficient kg/m ² /s	Vapour diffusion resistance factor - relative humidity dependent		Thermal conductivity - moisture dependent		Thermal conductivity - temperature dependent
						Relative humidity dimensionless	Water content kg/m ³		Relative humidity dimensionless	mu-value dimensionless	Water content kg/m ³	Thermal conductivity W/mK	Temp °C	Thermal conductivity W/mK
2190	0.16	850*	1.5	30	17	0	0	0.086	0	30	0	1.5	20	1.5
						0.33	6.3	0.086	0.265	30	133	3.4		
						0.53	8.1		0.715	17				
						0.72	10.2		1	17				
						0.81	11.3							
						0.89	14.5							
						1	133							

*Assumed value, not measured

Table A5 - Craigleith sandstone.

Material	Craigleith sandstone					Any other information		Data from Heriot-Watt University						
	Bulk density kg/m ³	Porosity m ³ /m ³	Heat capacity J/kgK	Thermal conductivity dry W/mK	Vapour diffusion resistance factor - dry cup	Vapour diffusion resistance factor - wet cup	Moisture storage function		Water absorption coefficient kg/m ² /s	Vapour diffusion resistance factor - relative humidity dependent		Thermal conductivity - moisture dependent		Thermal conductivity - temperature dependent
						Relative humidity dimensionless	Water content kg/m ³		Relative humidity dimensionless	mu-value dimensionless	Water content kg/m ³	Thermal conductivity W/mK	Temp °C	Thermal conductivity W/mK
2450	0.08	850*	1.7	120	63	0	0	0.0081	0	120	0	1.7	20	1.7
						0.33	4.6		0.265	120	45	4.3		
						0.53	6.5		0.715	63				
						0.72	8.8		1	63				
						0.81	10.5							
						0.89	13.3							
						1	45.2							

*Assumed value, not measured

Table A6 - Craigleith (Feak) or Hailes sandstone.

Material	Craigleith (Feak) or Hailes sandstone					Any other information		Data from Heriot-Watt University						
	Bulk density kg/m ³	Porosity m ³ /m ³	Heat capacity J/kgK	Thermal conductivity dry W/mK	Vapour diffusion resistance factor - dry cup	Vapour diffusion resistance factor - wet cup	Moisture storage function		Water absorption coefficient kg/m ² /s	Vapour diffusion resistance factor - relative humidity dependent		Thermal conductivity - moisture dependent		Thermal conductivity - temperature dependent
						Relative humidity dimensionless	Water content kg/m ³		Relative humidity dimensionless	mu-value dimensionless	Water content kg/m ³	Thermal conductivity W/mK	Temp °C	Thermal conductivity W/mK
2300	0.13	850*	1.9	63	27	0	0	0.036	0	63	0	1.9	20	1.9
						0.33	2.5	0.036	0.265	63	89.5	5.6	20	1.9
						0.53	3.5		0.715	27				
						0.72	5.1		1	27				
						0.81	6.2							
						0.89	8.8							
						1	89.5							

*Assumed value, not measured

Table A7 - Giffnock sandstone.

Material	Giffnock sandstone					Any other information		Data from Heriot-Watt University						
	Bulk density kg/m ³	Porosity m ³ /m ³	Heat capacity J/kgK	Thermal conductivity dry W/mK	Vapour diffusion resistance factor - dry cup	Vapour diffusion resistance factor - wet cup	Moisture storage function		Water absorption coefficient kg/m ² /s	Vapour diffusion resistance factor - relative humidity dependent		Thermal conductivity - moisture dependent		Thermal conductivity - temperature dependent
						Relative humidity dimensionless	Water content kg/m ³		Relative humidity dimensionless	mu-value dimensionless	Water content kg/m ³	Thermal conductivity W/mK	Temp °C	Thermal conductivity W/mK
2210	0.21	850*	1.1	37	18	0	0	0.073	0	37	0	1.1	20	1.1
						0.33	3		0.265	37	119	4.2		
						0.53	4.5		0.715	18				
						0.72	9.5		1	18				
						0.81	14.1							
						0.89	23.2							
						1	119							

*Assumed value, not measured

Table A8 - Scottish whinstone.

Material	Scottish whinstone					Any other information		Data from Heriot-Watt University						
	Bulk density kg/m ³	Porosity m ³ /m ³	Heat capacity J/kgK	Thermal conductivity dry W/mK	Vapour diffusion resistance factor - dry cup	Vapour diffusion resistance factor - wet cup	Moisture storage function		Water absorption coefficient kg/m ² /s	Vapour diffusion resistance factor - relative humidity dependent		Thermal conductivity - moisture dependent		Thermal conductivity - temperature dependent
						Relative humidity dimensionless	Water content kg/m ³		Relative humidity dimensionless	mu-value dimensionless	Water content kg/m ³	Thermal conductivity W/mK	Temp °C	Thermal conductivity W/mK
2920	0.02	850*	1.4	2200	580	0	0	0.0022	0	2200	0	1.4	20	1.4
						0.33			0.265	2200	6.1	2.4		
						0.53			0.715	580				
						0.72			1	580				
						0.81								
						0.89								
						1	6.1							

*Assumed value, not measured

Table A9 - Crathes granodiorite.

Material	Crathes granodiorite					Any other information		Data from Heriot-Watt University						
	Bulk density kg/m ³	Porosity m ³ /m ³	Heat capacity J/kgK	Thermal conductivity dry W/mK	Vapour diffusion resistance factor - dry cup	Vapour diffusion resistance factor - wet cup	Moisture storage function		Water absorption coefficient kg/m ² /s	Vapour diffusion resistance factor - relative humidity dependent		Thermal conductivity - moisture dependent		Thermal conductivity - temperature dependent
						Relative humidity dimensionless	Water content kg/m ³		Relative humidity dimensionless	mu-value dimensionless	Water content kg/m ³	Thermal conductivity W/mK	Temp °C	Thermal conductivity W/mK
2650	0.01	850*	2.1	1050	500	0	0	0.0011	0	1050	0	2.1	20	2.1
						0.33	2		0.265	1050	5.6	2.8		
						0.53	2.8		0.715	500				
						0.72	2.8		1	500				
						0.81	2.9							
						0.89	3.1							
						1	5.6							

*Assumed value, not measured



HISTORIC
ENVIRONMENT
SCOTLAND

ÀRAINNEACHD
EACHDRAIDHEIL
ALBA

Historic Environment Scotland
Longmore House, Salisbury Place
Edinburgh EH9 1SH

0131 668 8600
historicenvironment.scot

Historic Environment Scotland – Scottish Charity No. SC045925
Registered Address: Longmore House, Salisbury Place, Edinburgh EH9
1SH